



Forced degradation study of efonidipine HCl ethanolate, characterization of degradation products by LC-Q-TOF-MS and NMR

Charu P. Pandya, Sadhana J. Rajput*

Department of Pharmaceutical Quality Assurance, Faculty of Pharmacy, The Maharaja Sayajirao University of Baroda, Center of Relevance and Excellence in New Drug Delivery System, Government of India, Vadodara, Gujarat, India.

ARTICLE INFO

Received on: 23/09/2019
Accepted on: 24/12/2019
Available online: 04/04/2020

Key words:

Forced degradation, efonidipine, preparative HPLC, LC-Q-TOF-MS, NMR and IR.

ABSTRACT

Efonidipine HCl Ethanolate is an antihypertensive drug with 1,4 dihydropyridine and phosphinane derivative. Forced degradation study was performed in Efonidipine as per the guidelines by International Conference on Harmonization (ICH) Q1A (R2). Extensive degradation and slight degradation were observed in alkaline and photolytic conditions, respectively, whereas acidic, oxidative, and thermal conditions did not show any degradation. Degradation products were separated on Thermo Hypersil BDS C18 column (250 × 4.6 mm, 5 μ), mobile phase in gradient mode using ammonium acetate buffer and acetonitrile with detection at a wavelength of 254 nm. Six degradation products in alkaline condition and four degradation products in photolytic condition were identified by HPLC and characterized by mass spectrometry using LC-Q-TOF-MS, and degradation pathway was proposed. This is the typical case of degradation, where co-solvent methanol reacts with Efonidipine to form pseudo degradation products such as DP1, DP4, DP5, and DP6. Three degradation products DP1, DP3, and DP4 in alkaline condition were isolated by preparative HPLC and were characterized by LC-Q-TOF-MS, ¹H/¹³C NMR, and IR techniques. By characterization with these techniques, DP1 is characterized as 3-(2-(N-benzylanilino)ethyl 3-oxo-2,2-dimethylpropyl hydrogen 1,4-dihydro-2,6-dimethyl-4-(3-nitrophenyl) pyridin-3-yl-3-phosphonate, DP3 is characterized as 2-(N-benzyl-N-phenylamino) ethanol, and DP4 is characterized as 3-methoxy-2,2-dimethylpropyl hydrogen 1,4-dihydro-2,6-dimethyl-5-methyloxycarbonyl-4-(3-nitro)phenylpyridin-3-yl-3-phosphonate. The developed method was validated as per guidelines by ICH with respect to linearity, accuracy, precision, limit of detection, and robustness.

INTRODUCTION

Efonidipine HCL Ethanolate (EFO) is a new calcium channel blocker with dihydropyridine and phosphinane derivative. It blocks both T-type and L-type calcium channels (Hikaru and Koki, 2002; Masuda and Tanaka, 1994; Nakano *et al.*, 2010). It has a slow onset and longer duration of action. In a patient with essential hypertension, it causes an increase in renal blood flow, a

decrease in renal vascular resistance, and an increase in glomerular filtration rate. It chemically consists of 2-(N-benzylanilino) ethyl 5-(5, 5-dimethyl-2-oxo-1, 3, 2[^]5}-dioxaphosphinan-2-yl)-2, 6-dimethyl-4-(3-nitrophenyl)-1, 4-dihydropyridine-3-carboxylate, ethanol, hydrochloride with molecular formula C₃₆H₄₅ClN₃O₈P, and molecular weight 714.19 g/mole (Pubchem, 2019). Efonidipine has pKa (basic) of 2.33 and log P is 5.35 (Drugbank, 2019). It was approved in 1995 as a brand name Landel[®]. It is approved for marketing in India by Drug controller general India to Zuventus Pharma as Efnocar[®]. The HPLC method development of EFO has been reported (Kumar *et al.*, 2017). The LC-MS/MS method has been reported for the development of EFO in human plasma for pharmacokinetic applications and its stereospecific determination (Liu *et al.*, 2015; 2016). Literature has been reported on spectroscopic studies on the interaction of efonidipine with bovine serum albumin (Wang *et al.*, 2008), and the development considerations

*Corresponding Author
Sadhana J. Rajput, Department of Pharmaceutical Quality Assurance,
Faculty of Pharmacy, The Maharaja Sayajirao University of Baroda,
Center of Relevance and Excellence in New Drug Delivery System,
Government of India, Vadodara, Gujarat, India.
E-mail: sjrajput@gmail.com

for ethanolate with respect to stability and physicochemical considerations of EFO have been reported (Otsuka *et al.*, 2015). Solid dispersions of Efonidipine hydrochloride ethanolate with improved physicochemical and pharmacokinetic properties using microwave treatment have been reported (Otsuka *et al.*, 2016).

Chemical stability of the molecule is an important aspect since it affects the safety and efficacy of the product. There is a requirement of stability testing data from FDA and International Conference on Harmonization (ICH) guidance on how the quality of drug substance and drug product changes with time under the influence of environmental factors. In steps of controlling impurities or degradation products, their identification and characterization are the two main steps. These are performed when impurities or degradation products are present at the prescribed limits of 0.1% or even lower which are genotoxic in nature. The conventional approach comprises separation of degradation products by a suitable method and identification with the help of standard material. Alternative methods include enrichment or isolation and characterization through spectral techniques (Singh *et al.*, 2012). Sometimes it may not be possible to isolate the degradation products due to their low levels. Presently liquid chromatography/mass spectrometry and NMR techniques are the prominent techniques in structural identification and characterization of degradation products, which shows an important effect on evaluation safety aspects of drugs. The forced degradation helps in the possibility of generation of degradation products, thereby helps in determination of intrinsic stability of molecule and possibility of predicting degradation pathways and validation of stability indicating method (ICH Q1A (R2), 2003).

To the best of our knowledge, there are no reports on the forced degradation study on Efonidipine, identification, isolation, and characterization of degradation products. Our objective is to conduct the forced degradation study of Efonidipine to separate degradation products from Efonidipine, to identify and characterize the degradation products and isolate major degradation products by Preparative HPLC and its characterization using ^1H , ^{13}C NMR and IR techniques, and finally validation of the developed method as per guidelines by ICH.

EXPERIMENTAL

Materials and reagents

EFO was purchased from Shouguang Qihang International Trade Co., China. EFNOCAR[®] tablet was purchased from the local pharmacy in India. Chemicals used in the analysis were Acetonitrile (HPLC grade), methanol (HPLC grade), and acetic acid (HPLC grade) and were purchased from Rankem Pvt. Ltd, Mumbai, India. Ammonium acetate (HPLC grade), sodium hydroxide, hydrochloric acid, and hydrogen peroxide were purchased from S.D. Fine Chemical Ltd, Mumbai, India.

Equipment and Chromatographic conditions

HPLC PDA analysis was carried out by Shimadzu (Shimadzu Corporation, Kyoto Japan) containing Shimadzu LC-20 AD pump (binary), Shimadzu PDA M-20A diode array detector, and Rheodyne 7725 injector valve with a fixed loop of 20 μl . LC solution software (Shimadzu Corporation, Japan) was used for data integration. Separation was carried out on Thermo Hypersil BDS C 18 Column (250 \times 4.6 mm i.d., 5 μ particle size). Analytes

were detected at 254 nm. Buffer used in the mobile phase was acetate buffer (10 mM), which was prepared by dissolving 770 mg of ammonium acetate in 1,000 ml of double-distilled water. The pH was adjusted to 5.8 with acetic acid. Before use, acetate buffer was filtered through 0.2 μ Nylon 6, 6 membrane filter. Mobile phase flow rate was kept at 1 ml min^{-1} , and the mobile phase was run in gradient program as (time/% Acetonitrile) 0/25, 6/25, 11/40, 35/50, 45/50, 50/53, and 60/53.

Preparative HPLC chromatographic separation was performed on Shimadzu (Shimadzu Corporation, Kyoto, Japan) chromatographic system equipped with the Shimadzu LC-20AP pump (binary) and Shimadzu SPD-20A UV-visible detector. Samples were injected through the Rheodyne 7725 injector valve. Data acquisition and integration were performed using Class VP software. Phenomenex Luna column C 18 (250 \times 50 mm, 10 μ) was used for isolation of degradation. The flow rate was kept at 50 ml min^{-1} . Detection was performed at 254 nm. The gradient program was (time/% Acetonitrile) 0/5, 90/40, and 120/80.

LC-Q-TOF-MS system (Agilent Technologies, Inc, United States) comprising 1290 Infinity UHPLC system, 1260 infinity Nano HPLC with Chipcube, and 6550 ifunnel Q-TOF. Chemstation-LC control software was used for mass spectroscopic studies.

NMR spectroscopy was performed using Bruker Avance II 400 MHz NMR spectrometer for characterization of ^1H and ^{13}C -NMR spectra having dual broadband probe and z -axis gradients. Solvent used for NMR spectra was DMSO- d_6 , and the internal standard used was tetramethyl silane. Attached Proton test in ^{13}C NMR was conducted to confirm the presence of methyl and methine groups as positive peaks and methylene and quaternary carbon as negative peaks.

IR spectra were recorded on an 8400s spectrophotometer.

Precision water baths (Thermal Lining Services, Vadodara, India) with a temperature controller were used for degradation studies.

Photodegradation studies were performed in a photostability chamber (Thermolab Scientific Equipments Pvt. Ltd., Vadodara, India) with a light bank containing four UV (Osram L73) and fluorescent (L20) lamps (ICH Q1B, 1996).

PREPARATION OF EFO STOCK SOLUTION

Stock solution of 1 mg ml^{-1} was prepared by dissolving 25 mg of EFO in 25 ml of acetonitrile. From this solution, concentration in the range from 20 μg ml^{-1} to 120 μg ml^{-1} was prepared for linearity by dissolving 0.2, 0.4, 0.6, 0.8, 1.0, and 1.2 ml of stock solution in 10 ml of volumetric flask and making up to volume with the mobile phase (acetate buffer and acetonitrile 50:50).

FORCED DEGRADATION STUDY AND PREPARATION OF SAMPLE SOLUTIONS

Specificity of the method was determined by performing the forced degradation study of EFO by evaluating whether there is any impurity or degradation product is present in the analyte. EFO was subjected to hydrolytic, oxidative, thermal, and photolytic conditions as per the conditions prescribed by ICH guidelines. For the forced degradation study, initially, acetonitrile was added as a co-solvent but in alkaline degradation sample, the precipitate was obtained with acetonitrile so methanol was used as a

co-solvent since EFO was insoluble in stressor reagents and water (Singh and Bakshi, 2000). EFO stock solutions (1 mg ml^{-1}) were prepared in methanol. These stock solutions were diluted with 1 M HCl, 0.5 M NaOH, and 10% hydrogen peroxide (H_2O_2) in the ratio 1:1 (% v/v). Effect of dry heat (thermal degradation) was performed on solid state. EFO was spread in a Petri dish and kept in an oven at 80°C for 11 days under dry heat conditions. During photodegradation, solid drug powder and solution form were exposed to fluorescent light (1.25 million lux hours) and UV light (200 Whm^{-2}) in a photostability chamber. All the degradation samples (acid, base degradation samples were neutralized with 1 M NaOH and 0.5 M HCl) were diluted to a concentration of $100 \mu\text{g ml}^{-1}$ with the mobile phase (ammonium acetate buffer:acetonitrile 50:50).

VALIDATION OF DEVELOPED METHOD (ICH Q2(R1), 2005 AND FDA, 2000)

The method was developed as per ICH guidelines in terms of linearity, precision, limit of detection, limit of quantification, accuracy, and robustness.

System suitability tests were performed from six replicate injections of the drug solution. The result of each system suitability test was compared with the defined acceptance criteria. Retention factor, tailing factor ($T \leq 2.0$), theoretical plates ($N > 2,000$), and %RSD were evaluated for results. For linearity, solutions in the concentration ranging from $20 \mu\text{g ml}^{-1}$ to $120 \mu\text{g ml}^{-1}$ were injected into the HPLC system. Linearity sample was injected in triplicate. Peak areas of the respective concentration were noted. Graph was prepared by plotting peak area versus concentration. Regression equation was obtained, and the value of r^2 was obtained from the regression equation. Precision was calculated by the repeatability method by evaluating in six different concentrations three times a day for intra-day precision and on three different days for inter-day precision. Twenty microliters of six different concentrations were injected, and the average of the peak areas and %RSD was calculated. Accuracy was performed by the standard addition method. A known amount of EFO sample solution of a concentration of $40 \mu\text{g ml}^{-1}$ was added to the standard solutions to obtain concentrations of 60, 80, and $100 \mu\text{g ml}^{-1}$. Recovery samples were prepared in triplicate and injected for analysis. Robustness was evaluated by analyzing deliberate changes in the method variables. The parameters taken for analysis were pH of buffer (5.8 ± 0.2 units), initial gradient ratio (2%), and flow rate ($1 \pm 0.1 \text{ ml min}^{-1}$).

ISOLATION OF DEGRADATION PRODUCTS IN ALKALINE CONDITIONS

Major degradation products formed were DP1, DP3, and DP4 in alkaline hydrolysis

Preparation of alkaline degradation samples – 1 g of EFO was added to 30 ml of methanol and 20 ml of 0.5 M NaOH. The solution for degradation was maintained at room temperature for 48 hours. The solution was neutralized and analyzed by HPLC. In alkaline hydrolysis, DP1, DP3, and DP4 are formed with 50%, 25%, and 10%, respectively, area by normalization.

Isolation of degraded samples by preparative HPLC – For purification, degradation products DP1, DP3, and DP4 were separated by preparative HPLC. Fractions of greater than 97% were collected together. The solutions were concentrated on

rotavapour to remove acetonitrile. To confirm the retention time of isolated impurity, isolated fraction was analyzed by HPLC. The solutions were dried in a lyophilizer. DP1, DP3, and DP4 were obtained as white solids.

RESULTS AND DISCUSSION

HPLC method development

To optimize the method, the trials were taken with water: methanol (50:50) and water: acetonitrile (50:50). Under these conditions, the peak was eluting late, and peak shape was broad with methanol. Other trials were taken with water: acetonitrile (35:65) and ammonium acetate buffer pH 5: acetonitrile. From this, ammonium acetate buffer pH 5: acetonitrile (35:65) was found suitable for optimization. During the development of the forced degradation study, degradation products were formed in alkaline conditions, and the degradation products (DP6-DP2) were co-eluting. In photolytic condition, one of the degradation products (DP8) was co-eluting with EFO peak. To separate the degradation products in alkaline degradation, pH range (3–6) was tried, and various trials with modification in the mobile phase ratio were tried in the isocratic phase with methanol. pH 5.8 was found to be suitable for separation of degradation products in alkaline condition, and DP2 and DP3 peaks were merged with the addition of methanol in the mobile phase. For separation of DP8 from EFO in photolytic condition, various trials of the gradient were performed and also taken on C-8 column to separate DP8 from EFO. Finally, separation of DP8 from EFO and separation of degradation products (DP6-DP2) in alkaline conditions were achieved on C-18 column with acetate buffer with pH 5.8 and acetonitrile with the gradient program as (time/% B) 0/25, 6/25, 11/40, 35/50, 45/50, 50/53, and 60/53. EFO was eluted at the retention time of 57.66 minutes (Fig. 1a). Various trials for separation of DP8 from EFO are shown in Table 1.

Validation of the developed method

System suitability testing is an integral part of the development method and was performed to evaluate the behavior

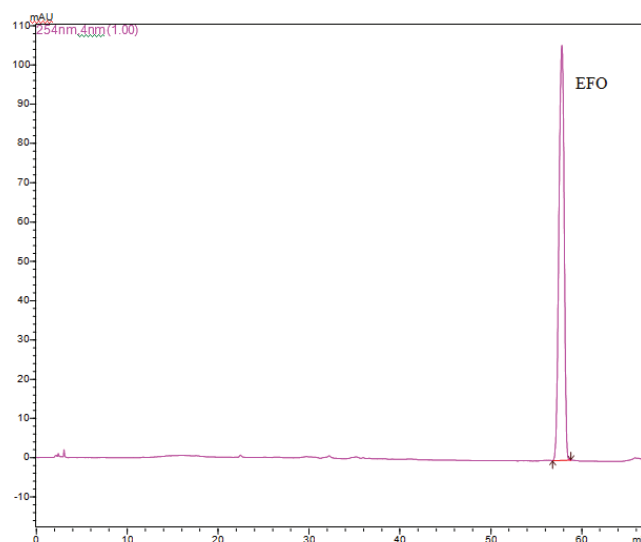


Figure 1a. Chromatogram of standard solution of EFO.

Table 1. Trials for separation of DP8 from EFO.

S.No.	Mobile Phase	EFO and DP8
1.	Gradient [Time (minutes)- % ACN] - 0.01-25, 6-25, 11-40, 30-65, 50-65, 51-25, 55-STOP	EFO Rt- 34.8 minutes, EFO and DP8 were co-eluting
2.	Gradient [Time (minutes)- % ACN] - 0.01-25, 6-25, 11-40, 25-65, 30-35, 40-35, 41-25, 45-STOP	EFO Rt- 35 minutes, EFO and DP8 were co-eluting
3.	Gradient [Time (minutes)- % ACN]- 0.01-25, 6-25, 11-40, 22-40, 30-55, 45-55, 46-25, 50-STOP	EFO Rt- 44.1 minutes, EFO and DP8 were co-eluting
4.	Gradient [Time (minutes)- % ACN]-0.01-25, 6-25, 11-40, 30-65, 50-65, 51-25, 55-STOP	EFO Rt- 34.6 minutes EFO and DP8 were co-eluting

of the chromatographic system. EFO eluted at 57.66 minutes. Tailing factor was less than 2 and theoretical plates were greater than 2,000. Linearity was calculated in the concentration range 20–120 $\mu\text{g ml}^{-1}$. Regression coefficient r^2 was found to be 0.9994 with the regression equation $y = 33223x + 15,744$. Based on the signal-to-noise ratio, the limit of detection was found to be 0.41 $\mu\text{g ml}^{-1}$, and the limit of quantification was found to be 1.24 $\mu\text{g ml}^{-1}$. Intraday and interday precision were calculated at six concentration levels 20–120 $\mu\text{g ml}^{-1}$. %RSD values of intraday and interday precision were found to be less than 2. The developed method was found to be precise. Recovery studies were performed by the standard addition method. % Recovery was found to be in the range of 99.7–100.25%. The developed method was accurate. Robustness was performed by analyzing slight changes in the method variables. The study was evaluated by changing the pH of buffer (5.8 ± 0.2 units), initial gradient ratio (2%), and flow rate ($1 \pm 0.1 \text{ ml min}^{-1}$) at a concentration of 40 $\mu\text{g ml}^{-1}$. The developed method was robust for all parameters. The results of system suitability parameters and validation parameters are shown in Table 2.

Forced degradation study

No degradation was observed when EFO was subjected to 1 M HCl at 80°C for 5 hours, 10% hydrogen peroxide at RT for 24 hours and dry heat at 80°C for 11 days. EFO when subjected to 0.5 M NaOH at room temperature for 6 hours, significant degradation (44.18%) was observed. There was a formation of six degradation products such as DP1 (28.14%), DP2 (4.01%), DP3 (8.8%), DP4 (2.17%), DP5 (0.66%), and DP6 (0.63%) at the retention time of 52.91 minutes, 26.66 minutes, 24.09 minutes, 20.29 minutes, 18.83 minutes, and 14.33 minutes (Fig. 1b). Slight degradation was observed in EFO and subjected to solution form in photolytic condition (11.6%) with the formation of degradation products DP10 (1.7%), DP9 (0.48%), DP8 (8.1%), and DP7 (0.98%) minutes at the retention time of 11.67 minutes, 30.01 minutes, 55.92 minutes, and 31.9 minutes, respectively (Fig. 1c).

From the above, it was observed that EFO was labile to alkaline and photolytic conditions in solution form, whereas it was stable in acidic, oxidative, and photolytic conditions in solid state.

Identification of degradation products by LC-Q-TOF-MS

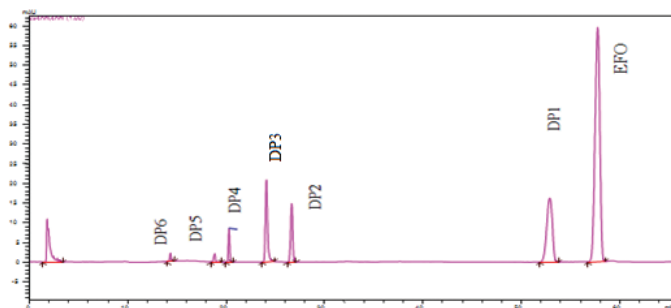
Degradation products formed in alkaline and photolytic conditions were identified by LC-ESI-Q-TOF-MS. High-resolution mass corresponding to the elemental composition of EFO and its DPs are shown in Table 3.

EFO – EFO is eluted at the retention time of 57.1 minutes. Molecular mass of Efonidipine HCl ethanolate is $\text{C}_{36}\text{H}_{45}\text{ClN}_3\text{O}_8$. EFO shows a corresponding mass of the Efonidipine base. Masses of HCl and Ethanolate are absent in mass spectra since their mass values are less than 50 m/z and ethanol is volatile so its mass is absent in mass spectra. The mass spectra of EFO show protonated

Table 2. System suitability and validation parameters of EFO.

System suitability Parameters	Value		
Retention Time (minutes \pm SD ^a)	57.66 \pm 0.05		
Tailing factor \pm SD ^a	0.94 \pm 0.007		
Theoretical Plates \pm SD ^a	69,040 \pm 424.06		
Validation Parameters	Value		
Calibration range	20–120 $\mu\text{g ml}^{-1}$		
LOD ($\mu\text{g ml}^{-1}$)	0.41		
LOQ ($\mu\text{g ml}^{-1}$)	1.24		
Regression Equation	$y = 33223x + 15744$		
Correlation coefficient	0.999		
Accuracy	% Recovery (Mean \pm SD ^a)		
50%	100.16 \pm 0.28		
100%	100.25 \pm 0.25		
150%	99.77 \pm 0.09		
Precision	%RSD ^b		
Intraday	1.20		
Interday	1.48		
Robustness			
Parameter	Levels	%RSD (Rt)	%RSD ^b (Area)
pH	5.6	0.87	0.15
	5.8	0.72	0.07
	6.0	0.75	0.18
Initial gradient ratio	23	0.37	0.14
	25	0.38	0.20
	27	0.48	0.10
Flow rate	0.9	0.51	0.12
	1.0	0.37	0.04
	1.1	0.39	0.03

a = Standard Deviation, b = % Relative Standard Deviation

**Figure 1b.** Chromatogram of alkaline degradation of EFO.

molecular ion at m/z 632 corresponds to molecular formula $\text{C}_{34}\text{H}_{38}\text{N}_3\text{O}_7$. EFO undergoes fragmentation at m/z 562 (loss of $\text{C}_4\text{H}_5\text{O}$ from m/z 632), 449 (loss of N-benzyl amino group from m/z 632), 405 (loss of ethoxy group from m/z 449), 337 (loss of

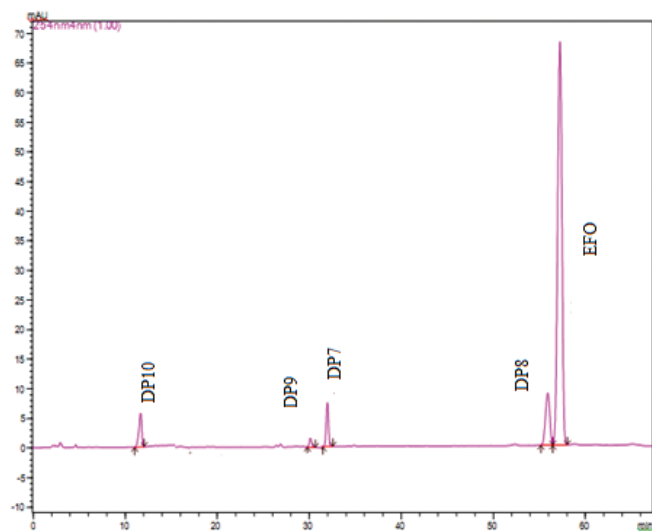


Figure 1c. Chromatogram of photolytic degradation (solution) of EFO.

C_5H_8 from m/z 405), and 210 (loss of $C_{19}H_{22}N_2O_7P^+$ from m/z 632) (Supple Figure S1a and b).

DP1 – DP1 is eluted at the retention time of 52.91 minutes. LC-ESI/MS/MS spectrum of DP1 shows protonated molecular ion at m/z 664 with the elemental composition of $C_{35}H_{42}N_3O_8P^+$. DP1 undergoes fragmentation to produce ions at m/z 608 (loss of C_3H_3O from 664), m/z 481 (loss of $C_{13}H_{12}N$ from m/z 664), m/z 437 (loss of $C_6H_{13}NO_6P$ from 664), m/z 351 (loss of $C_{17}H_{23}O$ from m/z 608), m/z 269 (loss of $C_{16}H_{23}N_2O_4P^+$ from 608), m/z 210 (loss of $C_{14}H_{13}NO_2^+$ from m/z 437), and m/z 181 (loss of C_2H_5 from m/z 210). DP1 formed by ring-opening of phosphinane and esterification by co-solvent methanol (Supple Figure S2a and b).

DP2 – DP2 is eluted at the retention time of 26.66 minutes. DP2 is formed with protonated molecular ion m/z 650 with the elemental composition of $C_{34}H_{41}N_3O_8P^+$. This mass is formed by ring-opening of phosphinane group (Supple Figure S3a).

DP3 – DP3 is eluted at the retention time of 24.06 minutes. DP3 is formed with protonated molecular ion m/z 228 with the elemental composition of $C_{15}H_{18}NO^+$. DP3 shows

Table 3. High-resolution mass data corresponding to the elemental composition of $[M+H]^+$ of EFO and its DPs.

Description	Retention Time	Molecular Formula	Observed Mass	Calculated Mass	Difference (ppm)		
EFO	57.33 minutes	$C_{34}H_{38}N_3O_7P^+$	632.2528	632.2514	1.4		
		$C_{30}H_{33}N_3O_6P^+$	562.3946	562.3101	-8.45		
		$C_{27}H_{32}N_2O_5P^+$	495.1718	495.2043	3.25		
		$C_{19}H_{22}N_2O_6P^+$	405.1172	405.122	-4.8		
		$C_{21}H_{26}N_2O_7P^+$	449.143	449.1474	-4.4		
		$C_{14}H_{14}N_2O_6P^+$	337.0544	337.0584	-4		
		$C_{15}H_{16}N^+$	210.126	210.1277	-1.7		
		$C_{35}H_{42}N_3O_8P^+$	664.278	664.2743	-0.37		
		$C_{32}H_{39}N_3O_7P^+$	608.3383	608.252	-8.63		
		$C_{22}H_{30}N_2O_8P^+$	481.1701	481.1734	0.33		
DP1	52.91 minutes	$C_{29}H_{29}N_2O_2^+$	437.144	437.1424	-0.16		
		$C_{15}H_{16}N_2O_6P^+$	351.0706	351.0778	0.72		
		$C_{16}H_{16}NO_3^+$	269.9899	270.1125	12.26		
		$C_{15}H_{16}N^+$	210.125	210.1277	0.27		
		$C_{13}H_{11}N$	181.0745	181.0891	1.46		
		DP2	26.66 minutes	$C_{34}H_{40}N_3O_8P^+$	650.2543	650.2587	-0.44
				$C_{15}H_{17}NO^+$	228.1373	228.1344	2.9
$C_{15}H_{15}N^+$	209.0322			209.0204	11.8		
$C_{13}H_{10}N^+$	180.066			180.0708	-4.8		
DP3	24.09 minutes	$C_{11}H_{14}N^+$	160.1093	160.1121	-2.8		
		$C_8H_{12}N^+$	122.0959	122.0964	-0.5		
		$C_7H_4N^+$	102.1275	102.1338	-6.3		
		$C_4H_8NO^+$	86.0965	86.0912	5.3		
DP4	20.29 minutes	$C_{21}H_{29}N_2O_8P^+$	469.1705	469.17	-0.05		
		$C_{20}H_{27}N_2O_6P$	422.0636	422.1607	9.71		
		$C_{15}H_{16}N_2O_6P^+$	351.0698	351.071	0.12		
		$C_{13}H_{11}N_2O_3^+$	243.002	243.074	7.2		
		$C_{15}H_{15}N_2O_3^+$	271.008	271.1077	9.97		
		$C_6H_{14}O_4P^+$	181.074	181.0624	-1.16		

Continued

Table 3. (Continued)

Description	Retention Time	Molecular Formula	Observed Mass	Calculated Mass	Difference (ppm)
DP5	18.83 minutes	$C_{20}H_{26}N_2O_7P^+$	437.1454	437.1433	-0.21
		$C_{19}H_{22}N_2O_6P^+$	405.1162	405.122	0.58
		$C_{19}H_{23}NO_4P^+$	360.1312	360.1359	0.47
		$C_{17}H_{22}NO_3P^+$	319.0424	319.0521	0.97
		$C_{17}H_{19}O_3P^+$	302.0366	302.1072	7.06
		$C_{19}H_{21}N_2O_5P^+$	388.1206	388.1188	-0.18
		$C_{14}H_{12}NO_2P^+$	257.0086	257.0606	5.2
		$C_{11}H_{13}NO_3P^+$	238.0012	238.0628	6.16
		$C_{11}H_{10}NOP^+$	203.0584	203.05	-0.84
		$C_9H_{10}OP^+$	164.9179	165.0464	12.85
DP6	14.33 minutes	C_7H_2OP	136.1128	136.0078	-10.5
		$C_{20}H_{28}N_2O_8P^+$	455.2	455.1505	-4.95
		$C_{27}H_{31}N_3O_7P^+$	540.1858	540.1855	0.55
		$C_{26}H_{29}N_3O_6P^+$	509.2001	509.1716	-2.85
		$C_{18}H_{21}N_2O_4P^+$	360.0288	360.1239	9.51
DP7	31.7 minutes	$C_8H_{10}N^+$	120.0793	120.0808	0.15
		$C_{10}H_{12}N^+$	145.0658	145.0891	2.33
		$C_{21}H_{24}N_2O_7P^+$	447.131	447.1399	-6.4
		$C_{19}H_{21}N_2O_7P^+$	421.1114	421.112	-2.3
		$C_{13}H_{17}NO_4P^+$	283.0462	283.0477	-5.2
		$C_8H_{13}NO_3P^+$	202.1781	202.1628	-1.53
		$C_{34}H_{37}N_3O_7P^+$	630.23	630.2324	-3.8
		$C_{32}H_{33}N_3O_6P^+$	586.2371	586.238	-1.53
		$C_{29}H_{26}N_3O_4P^+$	511.1617	511.1661	0.44
		$C_{21}H_{24}N_2O_7P^+$	447.128	447.1316	-3.47
DP8	55.92 minutes	$C_{19}H_{20}N_2O_6P^+$	403.1012	403.1026	-3.2
		$C_{19}H_{22}N_2O_4P^+$	373.1349	373.1312	-0.37
		$C_{16}H_{20}N_2O_4P^+$	335.0391	335.0402	-3.68
		$C_{16}H_{19}N_2O_2^+$	271.0699	271.0709	2.8
		$C_{15}H_{16}N^+$	210.1254	210.1244	1.1
		$C_7H_7^+$	91.0534	91.0542	0.08
		$C_{27}H_{33}N_3O_7P^+$	542.2017	542.2011	-7.6
		$C_{19}H_{22}N_2O_6P^+$	405.1167	405.121	-2.82
		$C_{17}H_{22}NO_3P^+$	319.0484	319.0493	0.09
		$C_7H_6N^+$	104.1087	104.0495	-5.92
DP10	11.67 minutes	$C_{28}H_{35}N_2O_5P^+$	510.212	510.2284	3.93

fragments of m/z 209 (loss of hydronium ion from m/z 228), m/z 180 (loss of ethyl group from m/z 209), m/z 160 (loss of C_4H from m/z 209), m/z 122 (loss of C_7H_6O from m/z 228), m/z 102 (loss of C_6H_6 from m/z 180), and m/z 86 (loss of $C_{11}H_{10}$ from m/z 228). DP3 is formed by hydrolysis at ester group of EFO with the loss of aromatic nitro group, 1, 4 dihydropyridine and cyclic phosphinane ring (Supple Figure S4a and b).

DP4 – DP4 is eluted at the retention time of 20.29 minutes. LC-ESI/MS/MS spectrum of DP4 shows protonated molecular ion peak at m/z 469 with the elemental composition of $C_{21}H_{29}N_2O_8P^+$. DP4 shows fragment ions of m/z 422 (loss of CH_2O_2) and m/z 271 (loss of $C_6H_{14}O_5P^+$). Fragment ion m/z 422 undergoes further fragmentation to produce ions at m/z 351 (loss of

C_5H_{11} from m/z 422), m/z 243 (loss of $C_2H_5O_3P$ from 351), and m/z 181 (loss of $C_{14}H_{13}N_2O_2$ from m/z 422) (Supple Figure S5a and b).

DP5 – DP5 is eluted at the retention time of 18.83 minutes. LC-ESI/MS/MS spectrum of DP5 shows protonated molecular ion peak at m/z 437 with the elemental composition of $C_{20}H_{26}N_2O_7P^+$. DP5 shows fragment ions of m/z 405 (loss of methoxy group from m/z 437), and m/z 388 (loss of from CH_3O_2 m/z 437). m/z 405 undergoes further fragmentation to produce ions of m/z 360 (loss of nitrous acid from m/z 405), m/z 319 (loss of C_2HO from m/z 360), m/z 302 (loss of NH_3 from m/z 319). Further fragmentation takes place at m/z 388 to produce ions of m/z 257 (loss of $C_5H_9NO_3$ from m/z 388), m/z 238 (loss of $C_8H_8NO_2$ from m/z 388), m/z 203 (loss of H_3O_2 from 238), m/z 164 (loss

of C_2N from m/z 203), and m/z 136 (loss of C_2H_5 from m/z 164) (Supple Figure S6a and b).

DP6 – DP6 is eluted at the retention time of 14.33 minutes. DP6 is formed with protonated molecular ion at m/z 455 with the elemental composition of $C_{20}H_{28}N_2O_8P^+$. It undergoes fragmentation by removal of methyl group to give m/z at 441 (Supple Figure S7a and b).

DP7 – DP7 is eluted at the retention time of 31.9 minutes. LC-ESI/MS/MS spectrum of DP7 shows protonated molecular ion peak at m/z 540 with the elemental composition of $C_{27}H_{31}N_3O_7P^+$. DP7 shows fragment ions of m/z 509 (loss of CH_2O from m/z 540) and m/z 447 (loss of C_6H_7N from m/z 540). Further fragmentation of m/z 509 gives to ions of m/z 360 (loss of $C_8H_8NO_2$ from m/z 540), m/z 120 (loss of $C_8H_8NO_2$ from m/z 509), and m/z 145 (loss of $C_8H_9NO_4P$ from m/z 360). Fragmentation of m/z 447 gives ions at m/z 421 (loss of C_2H_3 from m/z 447), m/z 283 (loss of $C_6H_4NO_3$ from m/z 421), and m/z 202 (loss of C_5H_4O from m/z 283). DP7 is formed by the loss of benzyl group from EFO (Supple Figure S8a and b).

DP8 – DP8 is eluted at the retention time of 55.92 minutes. LC-ESI/MS/MS spectrum of DP8 shows protonated molecular ion peak at m/z 630 with the elemental composition of $C_{27}H_{33}N_3O_7P^+$. DP8 shows protonated fragment ion at m/z 586 (loss of C_2H_4O from m/z 630). This fragment undergoes further fragmentation at m/z 511 (loss of $C_3H_7O_2$) and at m/z 373 (loss of $C_{13}H_{11}NO_2$). Fragment ion m/z 373 undergoes further fragmentation at m/z 335 (loss of C_3H_2 from m/z 373) and m/z 271 (loss of meta phosphoric acid from m/z 335). DP8 undergoes fragmentation to produce fragment ion at m/z 447 (loss of $C_{13}H_{13}N$), m/z 403 (loss of C_2H_4O from 447), m/z 210 (loss of $C_{19}H_{21}N_2O_7P$ from m/z 630), and m/z 91 (loss of C_8H_9N from m/z 210). DP8 is formed from EFO by dehydrogenation at a protonated m/z value of 630.23 (Supple Figure S9a and b).

DP9 – DP9 is eluted at the retention time of 30.01 minutes. LC-ESI/MS/MS spectrum of DP9 shows protonated molecular ion peak at m/z 542 with the elemental composition of $C_{27}H_{33}N_3O_7P^+$. DP9 shows fragment ions of m/z 405 (loss of $C_8H_{11}NOP$ from m/z 542), m/z 319 (loss of C_2NO_3 from m/z 405), and m/z 104 (loss of $C_{10}H_{16}O_3P$ from m/z 542). DP9 is formed by the loss of phenyl ethoxy amino group (Supple Figure S10a and b).

DP10 – DP10 is eluted at the retention time of 11.67 minutes and formed at m/z 510 with the elemental composition of $C_{28}H_{35}N_2O_5P^+$. DP10 is formed from the EFO by the removal of nitrophenyl group (Supple Figure S11a).

Degradation pathway of EFO

Alkaline condition – EFO possesses ester functional group and phosphinane ring. EFO in alkaline condition with the hydrolysis of phosphinane ring forms DP2. Hydrolysis of DP2 at phosphinane ring as a result there is ring-opening of phosphinane ring, and esterification with co-solvent methanol forms pseudo degradation product DP1, which on further hydrolysis at ester functional group forms pseudo degradation product DP4. DP4 on further hydrolysis at ester functional group forms pseudo degradation product DP6. EFO on direct hydrolysis at ester group forms DP3 and hydrolysis with esterification with co-solvent methanol forms pseudo degradation product DP5. Degradation of EFO in alkaline condition is shown in Figure 2a.

Photolytic condition – Under photolytic condition, EFO on dehydrogenation forms DP8 on which there is removal of benzyl group results in formation of DP7. EFO undergoes elimination of benzyl group forms DP9. EFO undergoes direct elimination of nitro phenyl group forms DP10. Degradation pathway of EFO in photolytic condition is shown in Figure 2b.

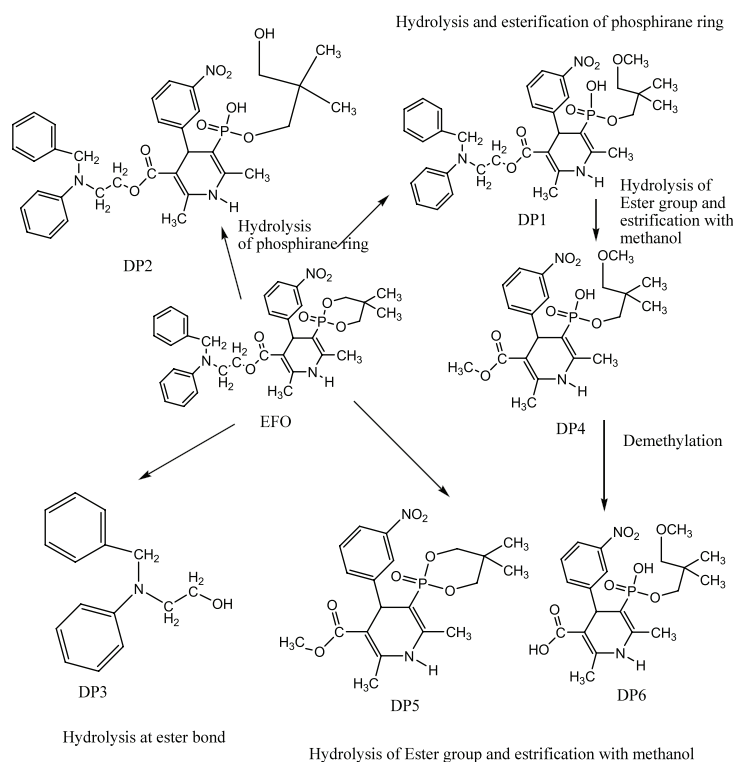


Figure 2a. Degradation pathway of EFO in alkaline condition.

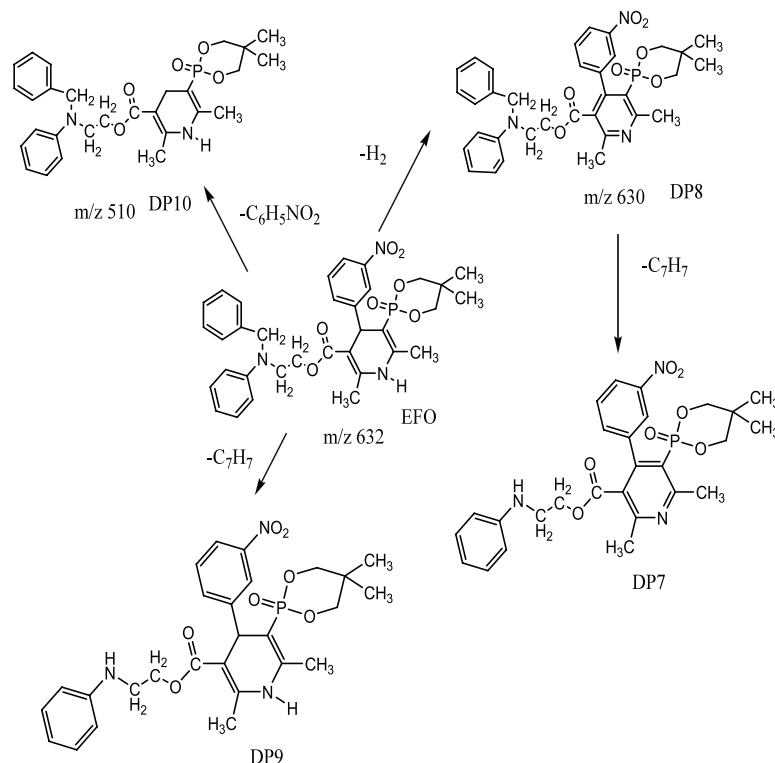


Figure 2b. Degradation pathway of EFO in photolytic condition.

Structural interpretation of isolated degradation products

Three degradation products such as DP1, DP3, and DP4 in alkaline conditions were isolated by preparative HPLC and subjected to NMR and IR analysis.

EFO – Structural analysis of EFO protonated mass at 632.2500 (calculated 632.2524). ¹H NMR spectra of EFO shows the presence of protons corresponding to methyl group at 0.87–0.86, 0.93, 2.20, and 2.27–2.26 ppm. The presence of protons corresponding to methylene groups is indicated at 4.58, 4.30–4.22, and 4.05–3.99 ppm. The presence of protons in aromatic nitro group is indicated at 8.0, 7.9, 7.5, and 7.4 ppm. Protons of ethanolate are present in the region of 1.07–1.05, 3.47–3.42, and 6.72 ppm. IR spectra of EFO show the presence of secondary amino group at 3,435 cm⁻¹ and the presence of aromatic groups at 3,185 and 3,083 cm⁻¹. The presence of methyl and methylene groups is indicated at 2,967 and 2,820 cm⁻¹. The presence of ester is indicated at 1,705 cm⁻¹ and cyclic ether linkage at 1,645 cm⁻¹ (Supple Table S1 and S5).

DP1 – Based on the analysis by LC-Q-TOF-MS, mass spectra of DP1 show protonated molecular ion peak at 664.2780 (calculated 664.2743), which is 32 amu more than that of EFO. This may be due to addition of methoxy group from co-solvent methanol. ¹H NMR spectra of DP1 were compared with that of EFO. In EFO, two methylene protons in phosphinane ring are indicated at 4.30–4.22 ppm and 4.05–3.99 ppm. In DP1, there is ring-opening of phosphinane ring, which is indicated by shifting of the methylene protons from 4.05–3.99 ppm to 3.34–3.31 ppm, and 3.55–3.51 ppm. Addition of three protons from methyl group is indicated by chemical shift at 3.42–3.35 ppm and the presence of one –OH group is indicated at 3.43–3.42 ppm. In ¹³C NMR spectra of DP1, methylene groups in phosphinane ring are shifted from 74 ppm to 69.89 ppm, and 66.41 ppm. Formation of additional methyl groups

is indicated at 51.35 ppm. This indicates opening of phosphinane ring and esterification by methanol. I.R spectrum of DP1 indicates formation of broad peak covering hydroxyl group and –NH group. Broad peak is observed in the bending region covering 1,705, 1,598, and 1,775 cm⁻¹. Peak at 1,645 cm⁻¹ in EFO has been disappeared in DP1 formation of the peak at 1,598 and 1,574 cm⁻¹ indicated ring-opening of phosphinane ring with formation of P-OH group and esterification with methanol. Thus DP1 is characterized as 3-2-(N-benzylanilino) ethyl 3-oxo-2,2-dimethylpropyl hydrogen 1,4-dihydro-2,6-dimethyl-4-(3-nitrophenyl)pyridin-3-yl-3-phosphonate (Supple Table S2 and S5).

DP3 – Based on the analysis by LC-Q-TOF-MS, mass spectra of DP3 show protonated molecular ion peak at 228.1373 (Calculated 228.1344). DP3 is 404 amu less than EFO. In DP3, there is an absence of four methyl protons at 0.87–0.86, 0.93, 2.20, and 2.27–2.26 and two methylene protons in phosphinane ring at 4.30–4.22 and 4.05–3.99, and absence of aromatic nitro group at 7.9, 8.0, 7.4, and 7.5 ppm. There is a formation of hydroxyl group which is indicated by a broad peak at 4.69 ppm. Protons at 15 and 16 position are shifted to upfield at 3.44–3.40 and 3.54–3.51 ppm.¹³C NMR of DP3 spectra indicates the absence of methyl groups and methylene groups at 17.48, 17.58, and 18.59 ppm. It indicates the absence of ester group at 166.41 ppm. From this, it indicates that hydrolysis has been taken at ester functional group with the loss of aromatic nitro group, dihydropyridine ring, phosphinane ring, and formation of phenyl benzyl ethanol. I.R. spectra of DP3 show the presence of a broad peak at 3,304 cm⁻¹. Aromatic ring is indicated by 3,000 cm⁻¹ and methyl group is indicated at 2,970 cm⁻¹. There is an absence of a peak at 1,705 cm⁻¹. Aromatic C–H bending is indicated by the appearance of a peak at 1,591 cm⁻¹. Based on this, DP3 is characterized as 2-(N-benzyl-N-phenyl amino) ethanol (Supple Table S3 and S5).

DP4 – Based on the analysis by LC-Q-TOF-MS, mass spectra of DP4 show protonated molecular ion peak at 469.1705 (Calculated 469.17). In DP4, there is an absence of two rings, which are indicated by the absence of peaks in the region from 6.3 to 7.14 ppm and absence of two methylene protons, which are indicated by the absence of a peak at 3.59 and 3.62 ppm. Formation of two methyl groups is indicated at 4.58, 4.30–4.22 ppm and there is a formation of one hydroxyl group at 3.33–3.28 ppm. One of the methylene groups is shifted to 3.63–3.51 ppm. ^{13}C NMR spectra of DP4 indicate the absence of aromatic rings and the absence of two methylene groups at 53 and 60 ppm. Esterification with methanol and formation of additional methyl group is indicated at 51.20 and 51.15 ppm. DP4 might have been formed from DP1 by hydrolysis at ester linkage with the loss of two aromatic rings and esterification with co-solvent methanol. IR spectra of DP4 indicate broad peak covering –OH group and –NH group. The presence of aromatic ring is indicated in the region of 3,192 and 3,166 cm^{-1} . Methyl groups are indicated in the region of 2,951, 2,873, and 2,848. Opening of phosphinane ring and further etherification by methanol is shown by ether linkage at 1,645 cm^{-1} . Based on the above analysis, DP4 is characterized as 3-methoxy-2,2-dimethylpropyl hydrogen 1,4-dihydro-2,6-dimethyl-5-methyloxycarbonyl-4-(3-nitro)phenylpyridin-3-yl-3-phosphonate (Supple Table S4 and S5).

Mechanism of formation of degradation products DP1, DP3, and DP4

DP1 – In alkaline condition, ring-opening of phosphinane takes place. Methoxide ion acts as nucleophile and it attacks on carbocation of phosphinane ring and forms the intermediate. Abstraction of a proton by negatively charged oxygen in the intermediate results in formation of DP1. Mechanism of formation of DP1 is shown in Figure 3a.

DP3 – EFO possess ester functional group. Nucleophilic attack of hydroxide ion takes place on ester. Cleavage of carbonyl bond takes place and tetrahedral intermediate is formed. Cleavage takes place at tetrahedral intermediate, there is a formation of 2-(N-benzyl-N-phenylamino) ethoxide ion. Abstraction of proton by 2-(N-benzyl-N-phenylamino) ethoxide ion results in formation of corresponding acid and DP3. Mechanism of formation of DP3 is shown in Figure 3b.

DP4 – DP4 is formed from DP1 by alkaline hydrolysis. In DP1, there nucleophilic attack of methoxide ion to carbonyl carbon and there is formation of tetrahedral intermediate. With further loss of benzyl phenyl ethyl amino group, there is a formation of DP4. Mechanism of formation of DP4 is shown in Figure 3c.

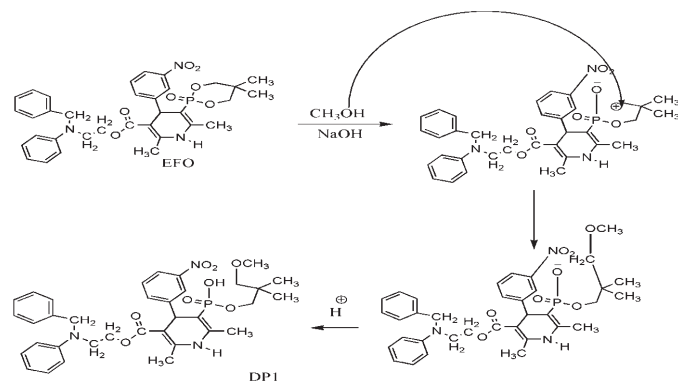


Figure 3a. Mechanism of formation of DP1.

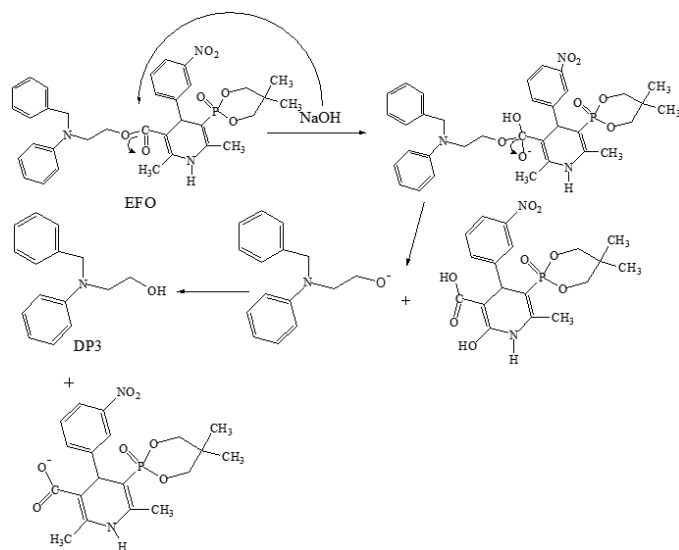


Figure 3b. Mechanism of formation of DP3.

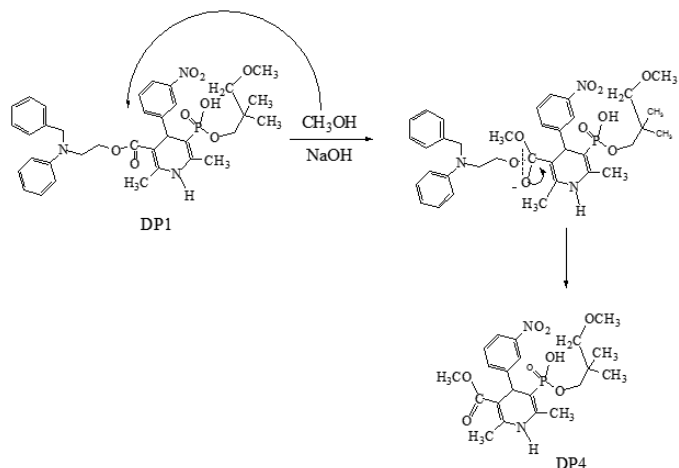


Figure 3c. Mechanism of formation of DP4.

CONCLUSION

Forced degradation study was performed for analysis of EFO. Degradation was observed in alkaline and photolytic conditions, and degradation products were identified by LC-ESI-Q-TOF-MS. Three degradation products in alkaline conditions were isolated by preparative HPLC and characterized by NMR and I.R. techniques. DP1 is characterized as 3-2-(N-benzylanilino)ethyl 3-oxo-2,2-dimethylpropyl hydrogen 1,4-dihydro-2,6-dimethyl-4-(3-nitrophenyl)pyridin-3-yl-3-phosphonate, DP3 is characterized as 2-(N-benzyl-N-phenylamino)ethanol, and DP4 is characterized as 3-methoxy-2,2-dimethylpropyl hydrogen 1,4-dihydro-2,6-dimethyl-5-methyloxycarbonyl-4-(3-nitro)phenylpyridin-3-yl-3-phosphonate. Degradation pathways in alkaline and photolytic conditions were proposed.

ACKNOWLEDGMENT

Charu Pandya is highly thankful to University Grants Commission, New Delhi and Government of India for availing Senior Research Fellowship [letter no. F.No. 25-1/2014-15(BSR)/7-129/2007(BSR)].

DECLARATION OF INTEREST

The authors declare that there is no conflicts regarding publication of this paper.

ABBREVIATIONS

ACN	Acetonitrile
BDS	Base Deactivated Silica
DP	Degradation Product
DMSO	Dimethyl sulphoxide
FDA	Food and Drug Administration
HPLC	High Performance Liquid Chromatography
ICH	International Conference on Harmonization
IR	Infra Red
LC-Q-TOF-MS	Liquid Chromatography Quadrupole Time of Flight Mass Spectrometer
LOD	Limit of Detection
LOQ	Limit of Quantification
NMR	Nuclear Magnetic Resonance
PDA	Photo Diode Array
RT	Room Temperature
RSD	Relative Standard Deviation

REFERENCES

- Drugbank.ca. 2019. Available via <https://www.drugbank.ca/drugs/DB09235>
- Food and Drug Administration (FDA). Guidance for industry: analytical procedures and methods validation. pp. 4–12, 2000.
- Hikaru T, Koki S. Efonidipine hydrochloride: a dual blocker of L- and T-type Ca(2+) channels. *Cardiovas Drug Rev* 2002; 20:81–92.
- International Conference on Harmonization (ICH). Guidance for industry: Q2(R1) validation of analytical procedures: text and methodology. pp. 6–13, 2005.
- International Conference on Harmonization (ICH). Q1A(R2) stability testing of new drug substances and products. pp. 5–16, 2003.
- International Conference on Harmonization (ICH). Q1B stability testing: photostability testing of new drug substances and products. pp. 4–6, 1996.
- Kumar A, Shoni SK, Dahiya M, Kumar R, Yadav AK, Kumar V, Choudhary H. Development and validation of liquid chromatography (RP-HPLC) methodology for estimation of Efonidipine HCl Ethanolate. *Pharm Anal Acta* 2017; 8:1–6.

Liu M, Deng M, Zhang D, Wang X, Ma J, Zhao H, Zhang L, Tong Y, Liu H. A chiral LC-MS/MS method for the stereo specific determination of efonidipine in human plasma. *J Biomed Pharm Anal* 2016; 122:35–41.

Liu M, Zhao H, Tong Y, Zhang D, Wang X, Zhang L, Han J, Liu H. 2015. Determination of efonidipine in human plasma by LC-MS/MS for pharmacokinetic applications. *J Pharm Biomed Anal* 2015; 103:1–6.

Masuda Y, Tanaka H. Efonidipine hydrochloride: a new calcium channel antagonist. *Cardiovas. Drugs Rev* 1994; 12:123–35.

Nakano N, Ishimitsu T, Takahashi T, Inada H, Okamura A, Ohba S, Matsuoka H. Effects of efonidipine, an L- and T-type calcium channel blocker, on the rennin-angiotension–aldosterone system in chronic hemodialysis patients. *Inter Heart J* 2010; 51:188–92.

National Center for Biotechnology Information. Pubchem Database. CID=163838. Available via <https://pubchem.ncbi.nlm.nih.gov/compound/Efonidipine-hydrochloride-ethanolate> (Accessed 4 December 2018).

Otsuka M, Maeno Y, Fukami T, Inoue M, Tagami T, Ozeki T. Development considerations for ethanolates with regard to stability and physicochemical characterization of efonidipine hydrochloride ethanolate. *Cryst Eng Comm* 2015; 17:743.

Otsuka M, Maeno Y, Fukami T, Inoue M, Tagami T, Ozeki T. Solid dispersions of efonidipine hydrochloride ethanolate with improved physicochemical and pharmacokinetic properties prepared with microwave treatment. *Euro. J Pharmaceu Biopharmaceu* 2016; 108:25–31.

Singh S, Bakshi M. Guidance on conduct of stress tests to determine inherent stability of drugs. *Pharmaceu Tech On-Line* 2000; 24:1–14.

Singh S, Handa T, Narayanam M, Sahu A, Junwal M, Shah RP. A critical review on the use of modern sophisticated hyphenated tools in the characterization of impurities and degradation products. *J Pharm Biomed Anal* 2012; 69:148–73.

Wang N, Ye L, Zhaon BQ, Yu JX. Spectroscopic studies on interaction of efonidipine with bovine serum albumin. *Brazilian J Med Bio Res* 2008; 41:589–95.

How to cite this article:

Pandya CP, Rajput SJ. Forced degradation study of efonidipine HCl ethanolate, characterization of degradation products by LC-Q-TOF-MS and NMR. *J Appl Pharm Sci*, 2020; 10(04):075–099.

SUPPLEMENTARY DATA

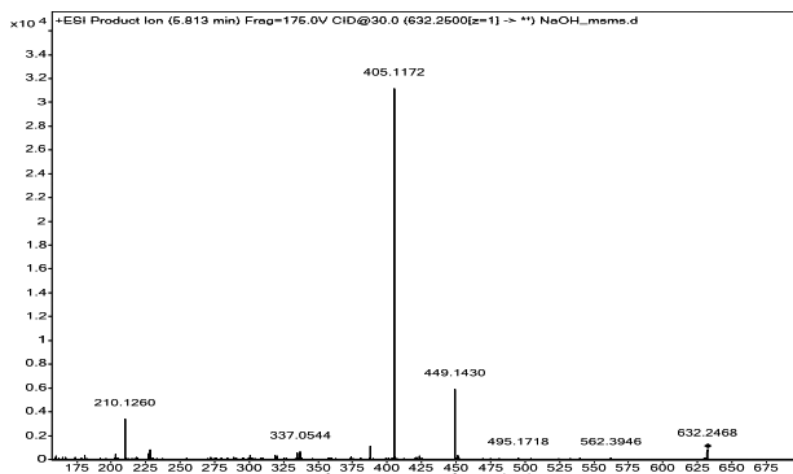


Figure. S1a . ESI-MS/MS spectra of EFO.

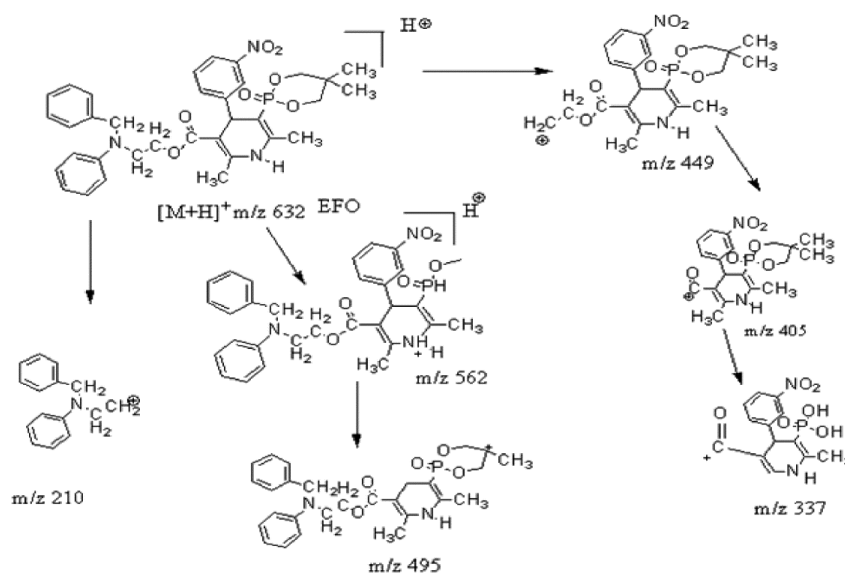


Figure. S1b. Fragmentation pathway of EFO.

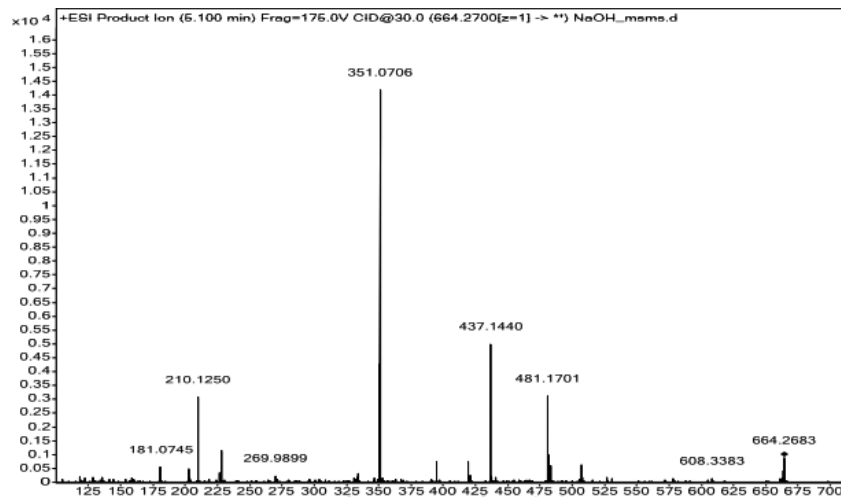


Figure. S2 -a. ESI-MS/MS spectra of DP1.

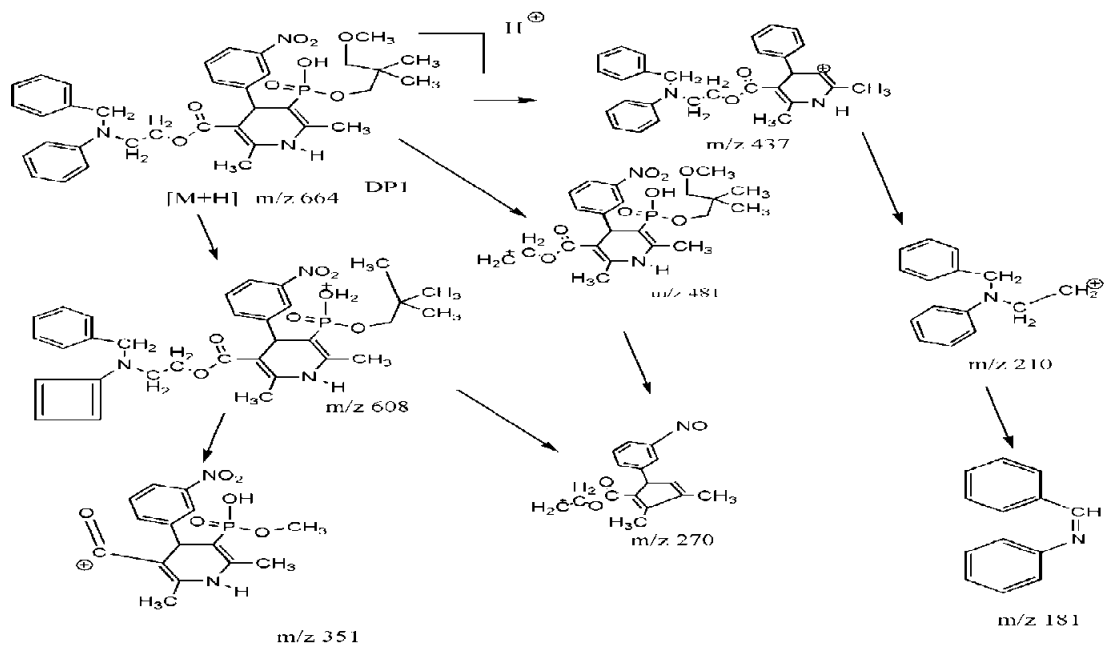


Figure. S2 b. Fragmentation pathway of DP1.

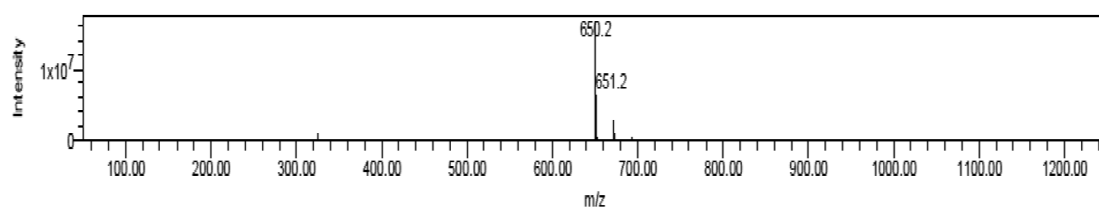


Figure. S3 a. ESI-MS spectra of DP2.

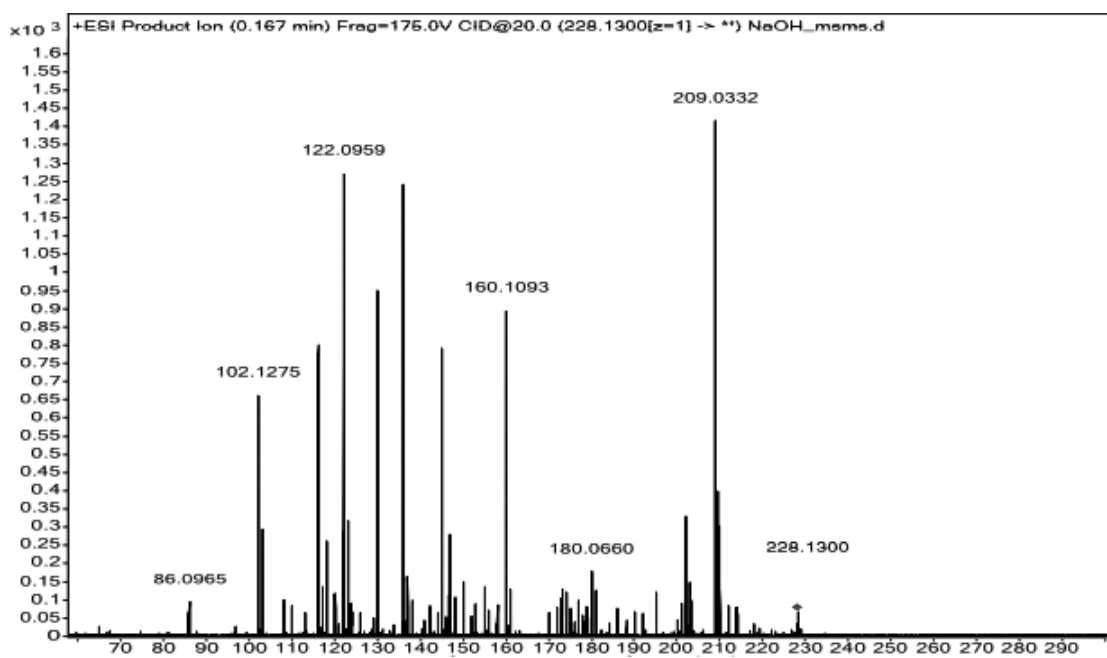


Figure. S4 a. ESI-MS/MS spectra of DP3.

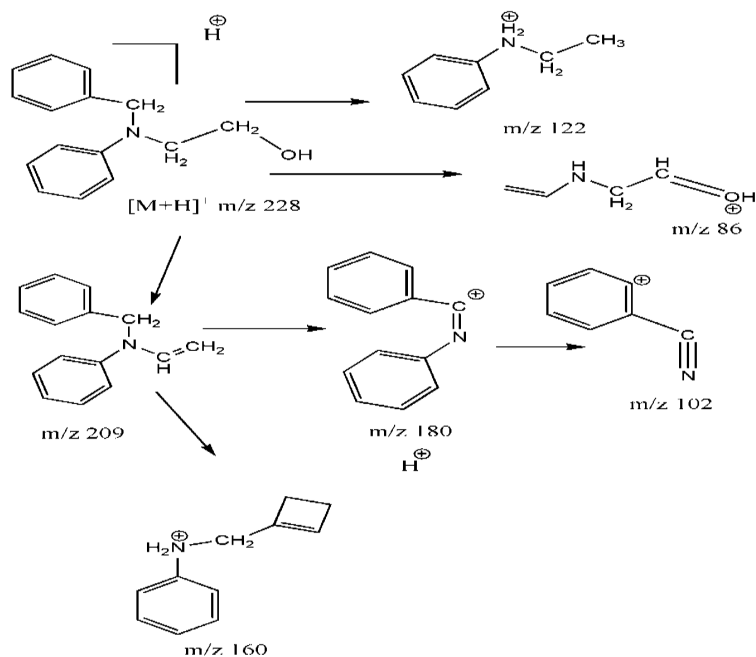


Figure. S4 b. Fragmentation pathway of DP3.

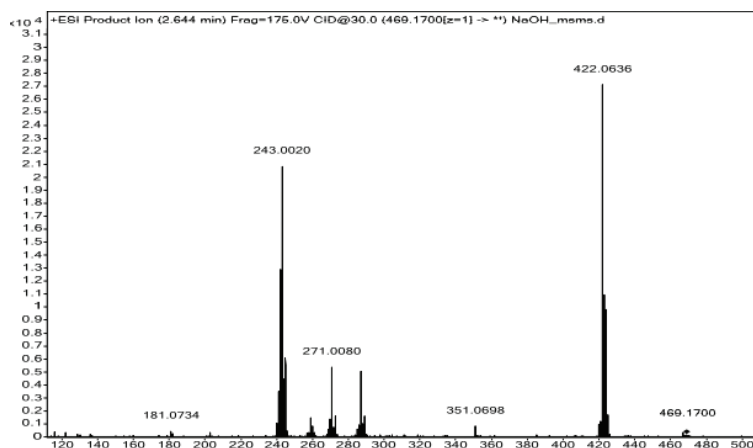


Figure. S5 a . ESI-MS/MS spectra of DP4.

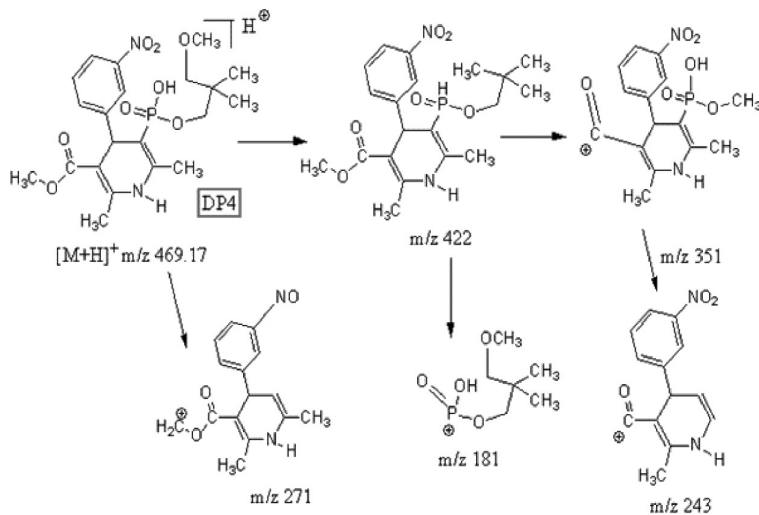


Figure. S5 b . Fragmentation pathway of DP4.

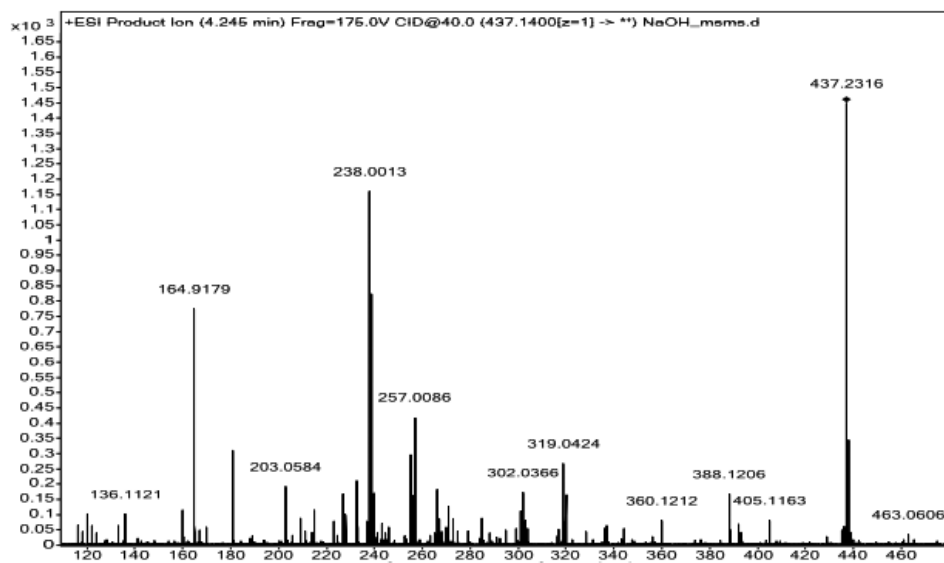


Figure. S6 a. ESI-MS/MS spectra of DP5.

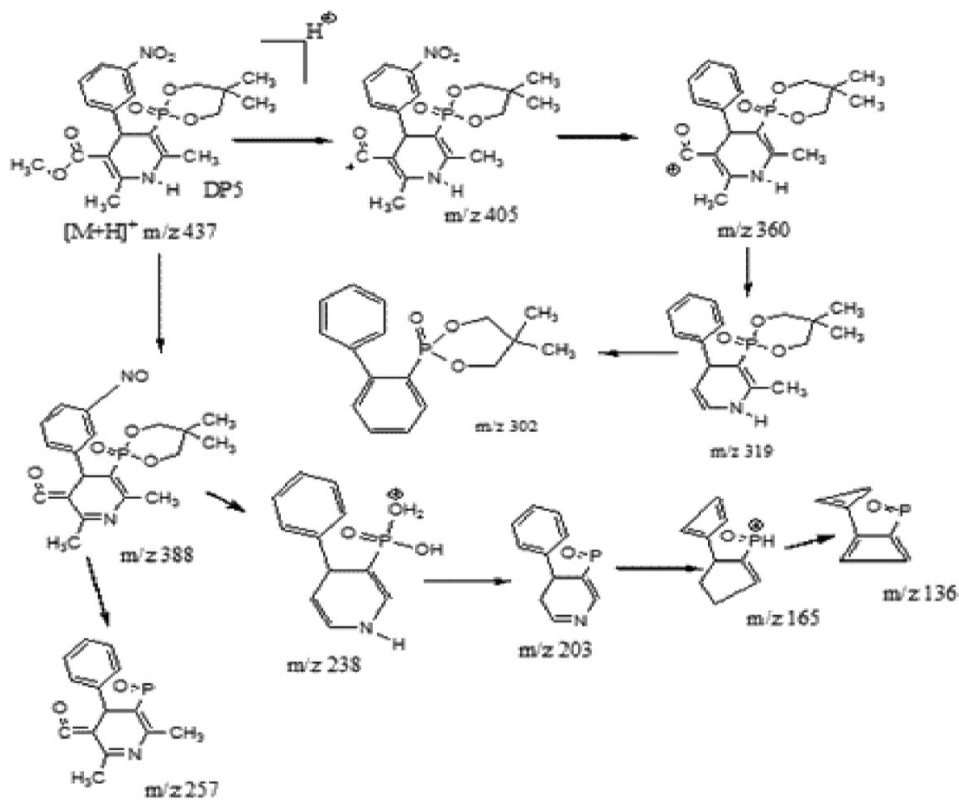


Figure. S6 b . Fragmentation pathway of DP5.

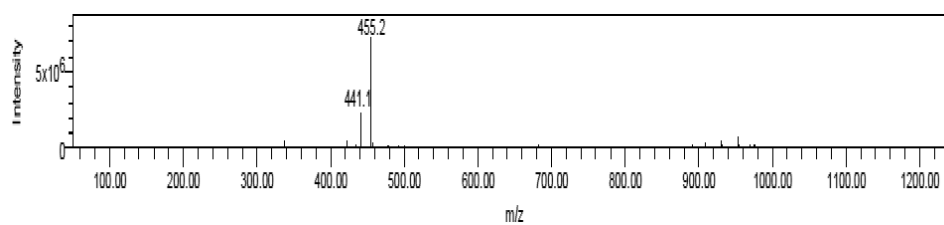


Figure.S7 a. ESI-MS spectra of DP6.

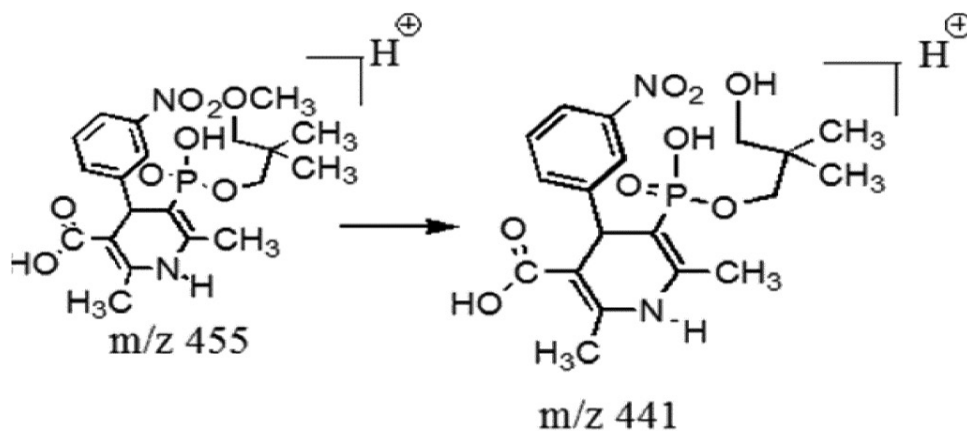


Figure.S7 b. Fragmentation pathway of DP6.

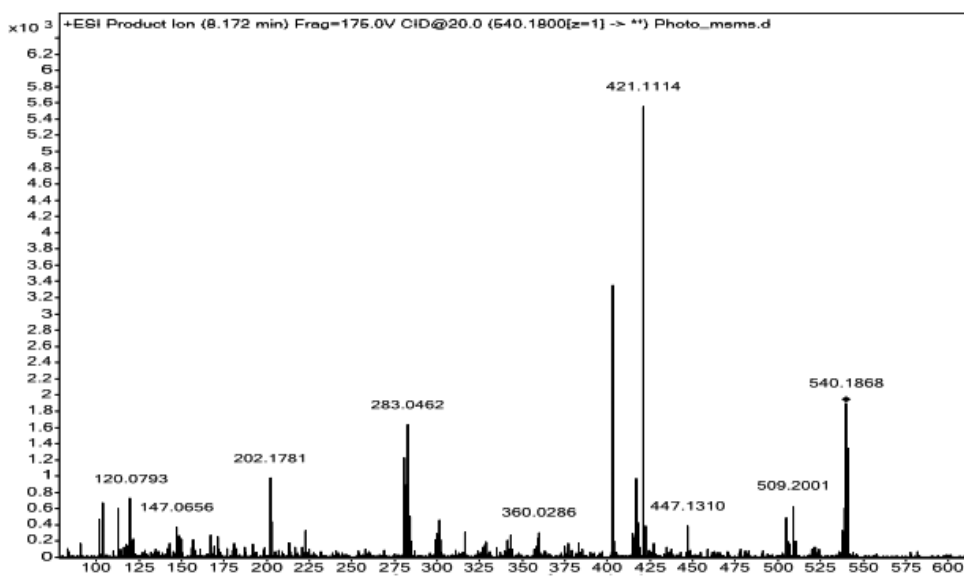


Figure. S8 a. ESI-MS/MS spectra of DP7.

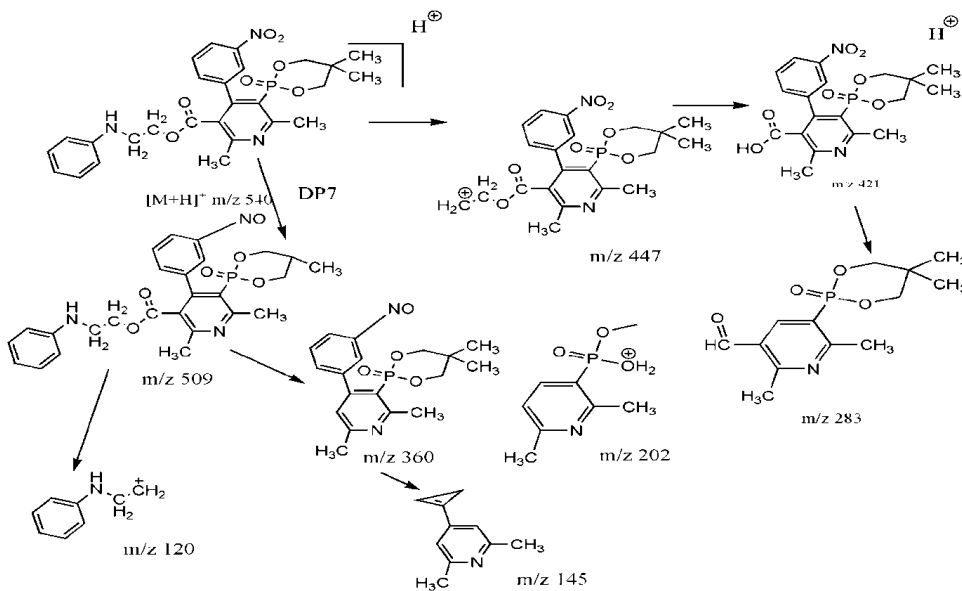


Figure. S8 b. Fragmentation pathway of DP7.

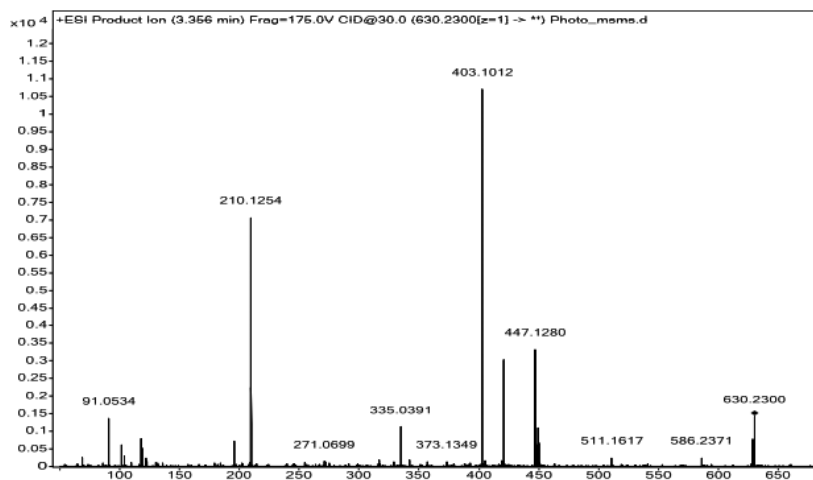


Figure. S9 a. ESI-MS/MS spectra of DP8.

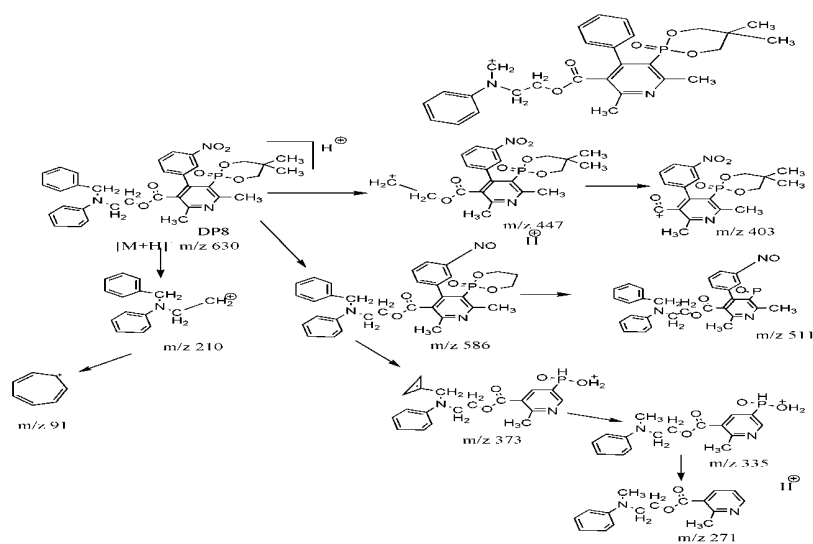


Figure. S9 b. Fragmentation pathway of DP8.

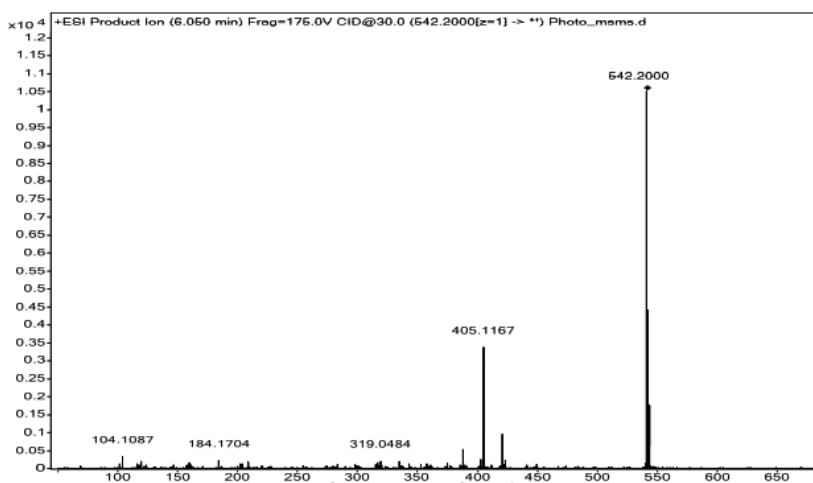


Figure. S10 a. ESI-MS/MS spectra of DP9.

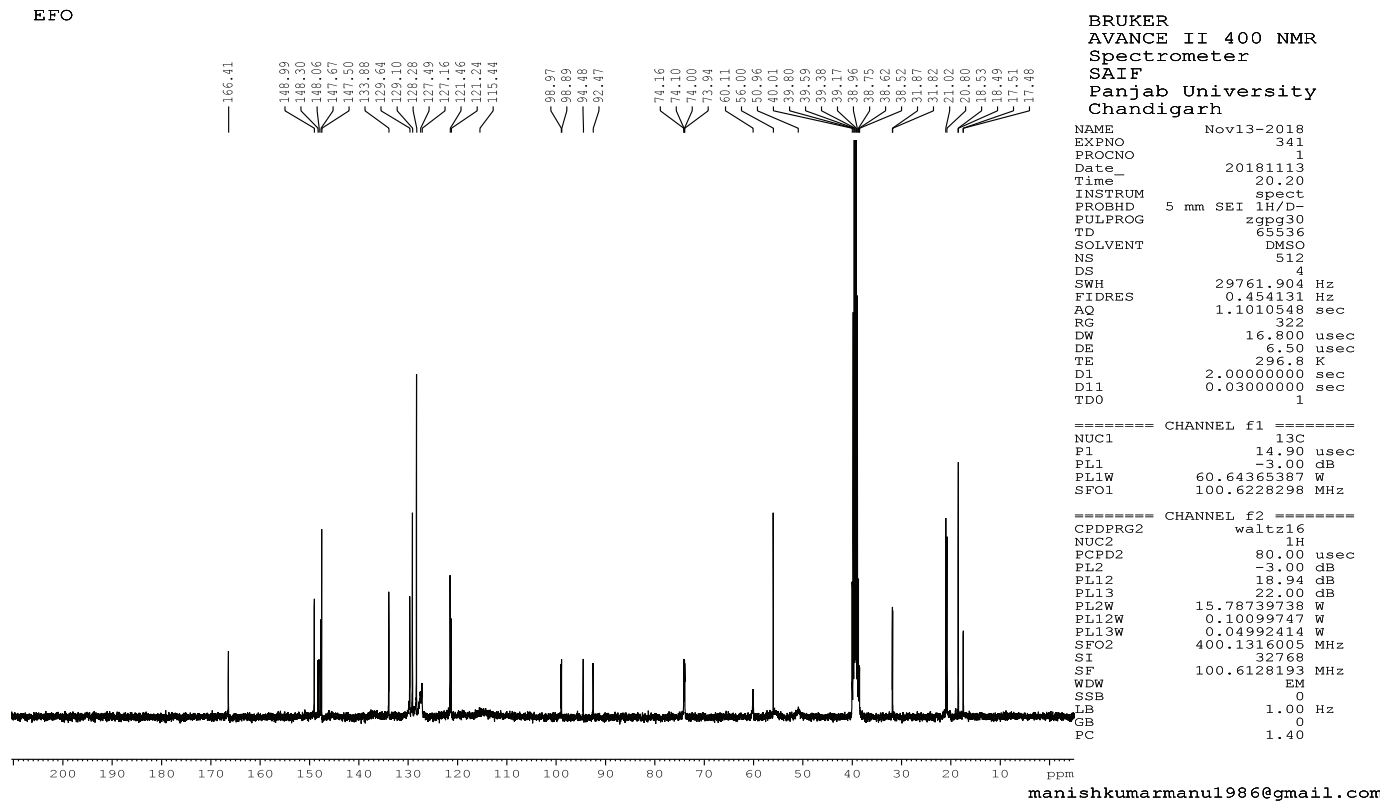
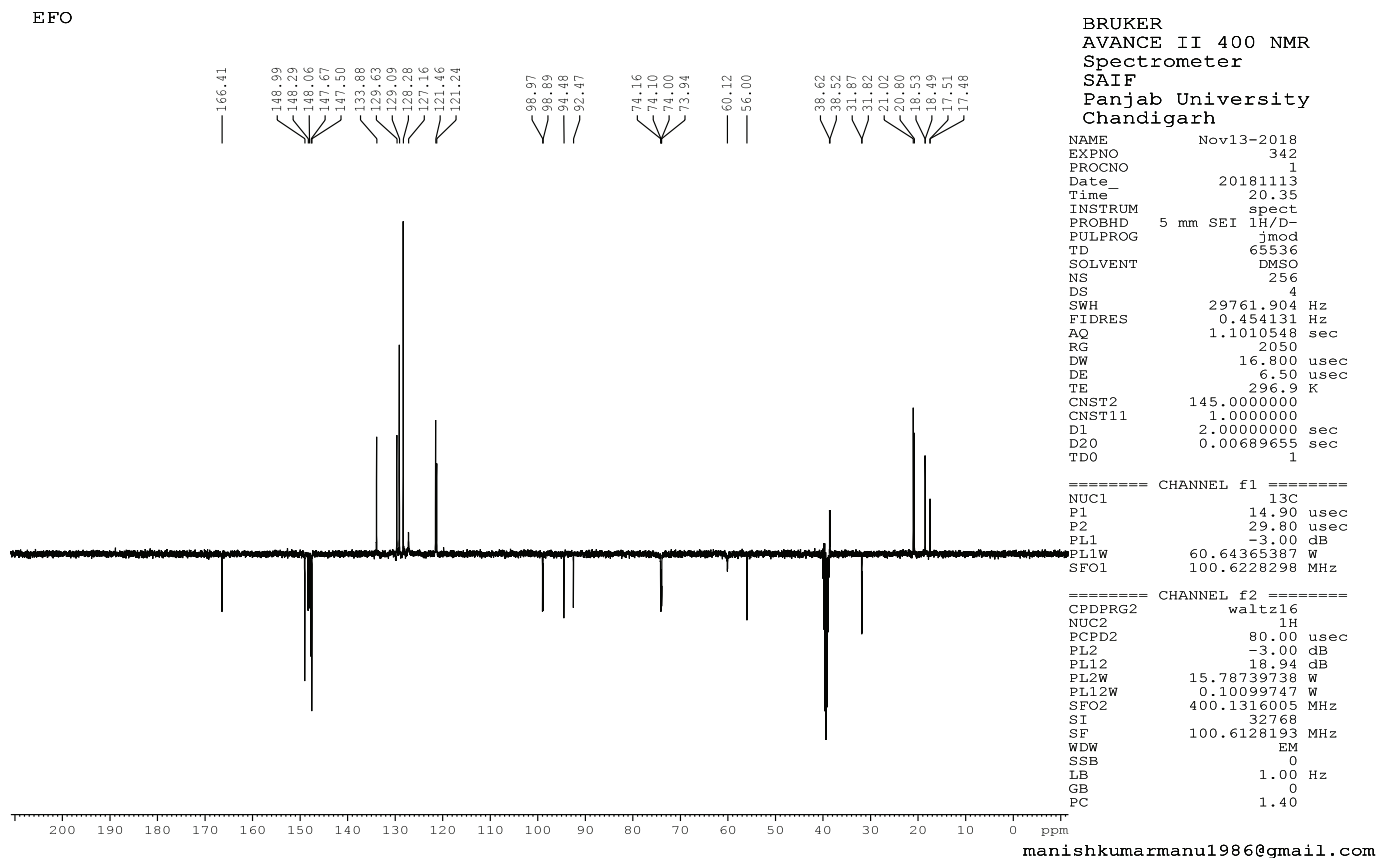
Figure. S12 b. ¹³C NMR spectra of EFO.

Figure. S12 c. APT spectra of EFO.

EFO

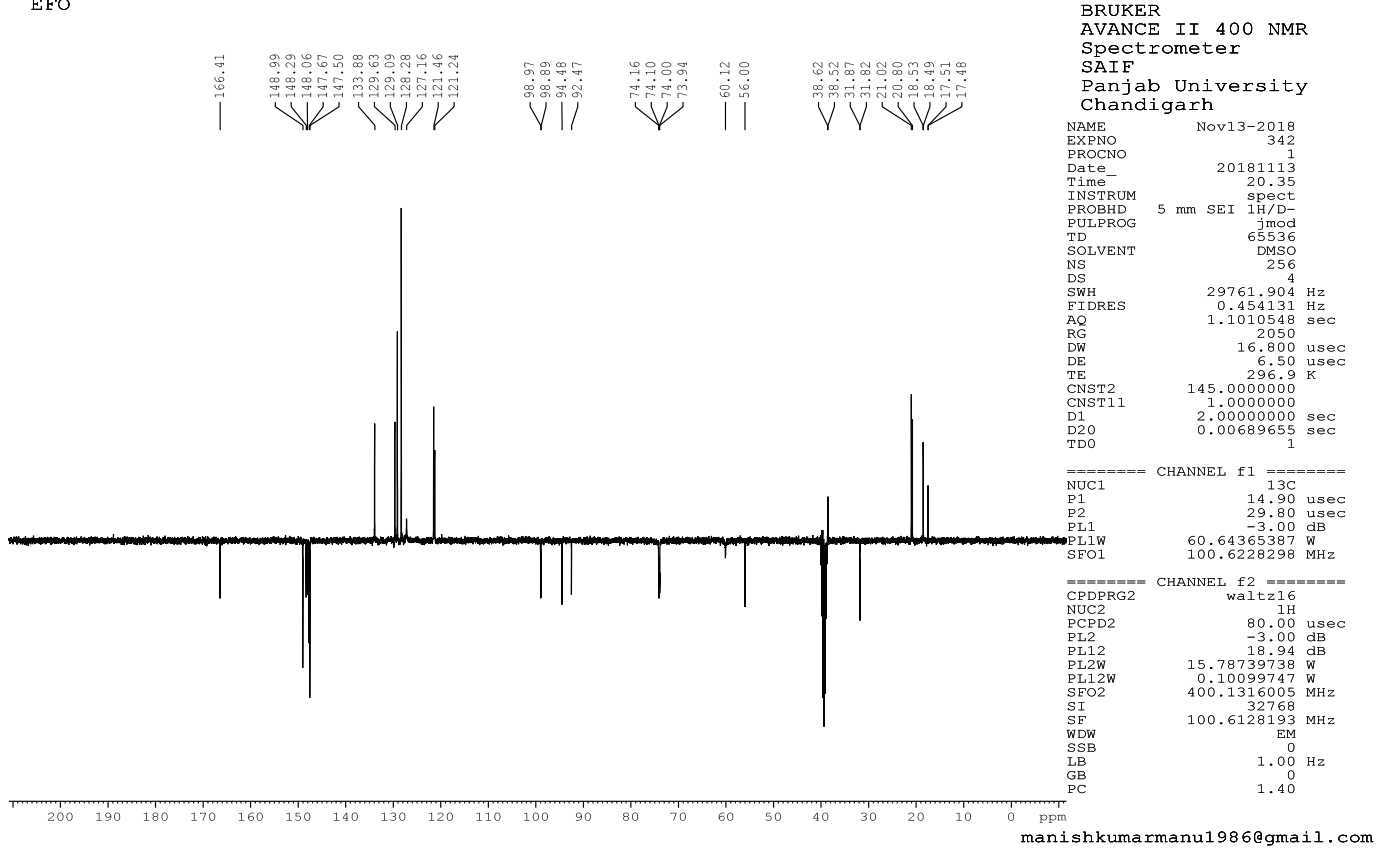


Figure. S13 a. ¹H NMR spectra of DP1.

EFO DP1

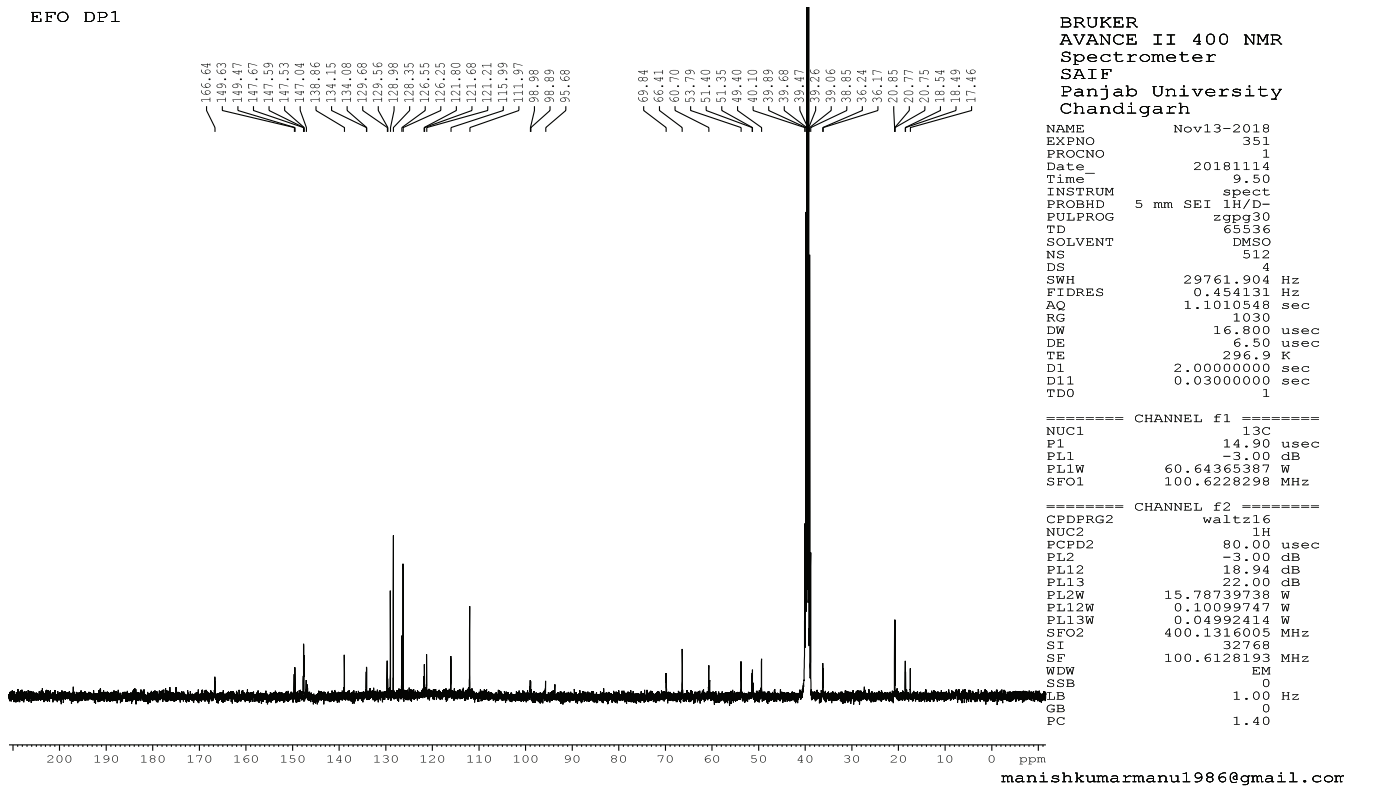


Figure. S13 b. ¹³C NMR spectra of DP1.

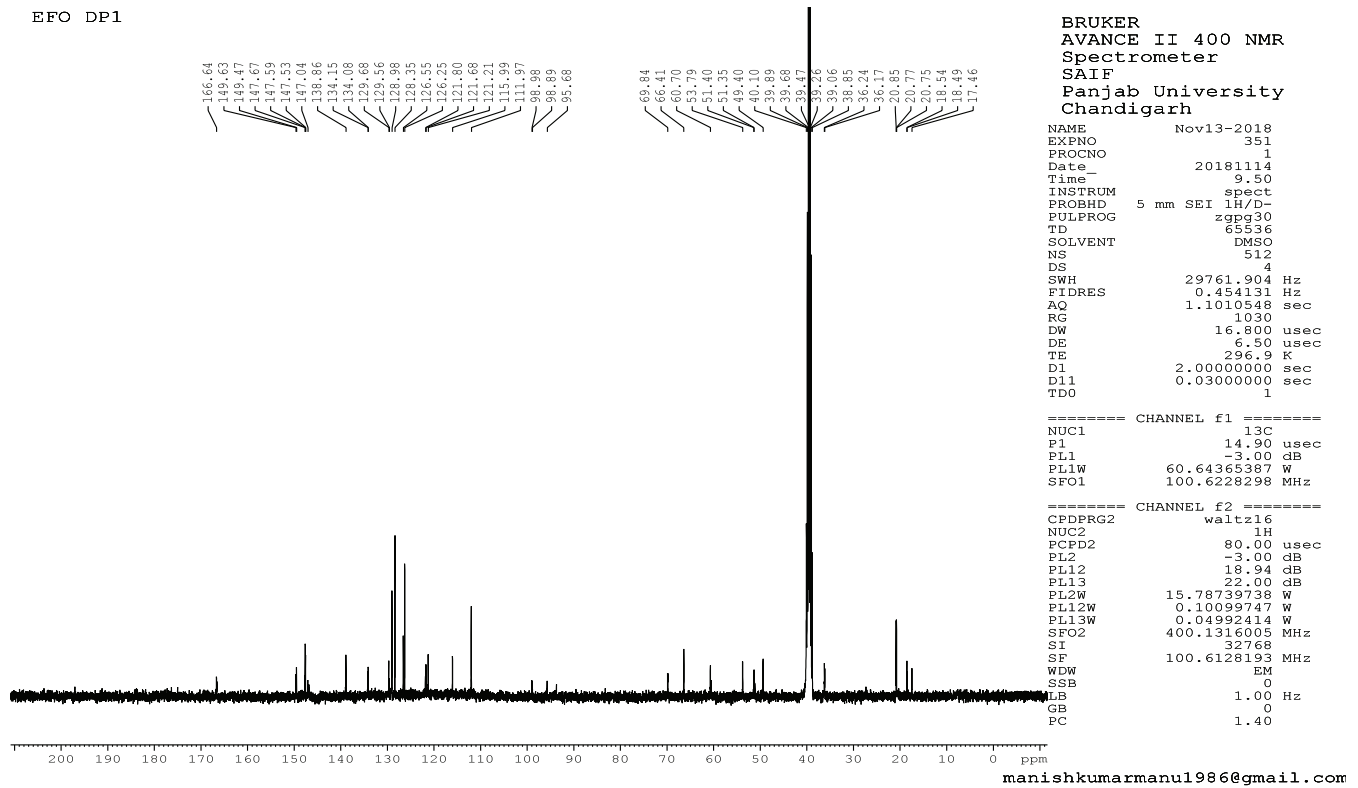
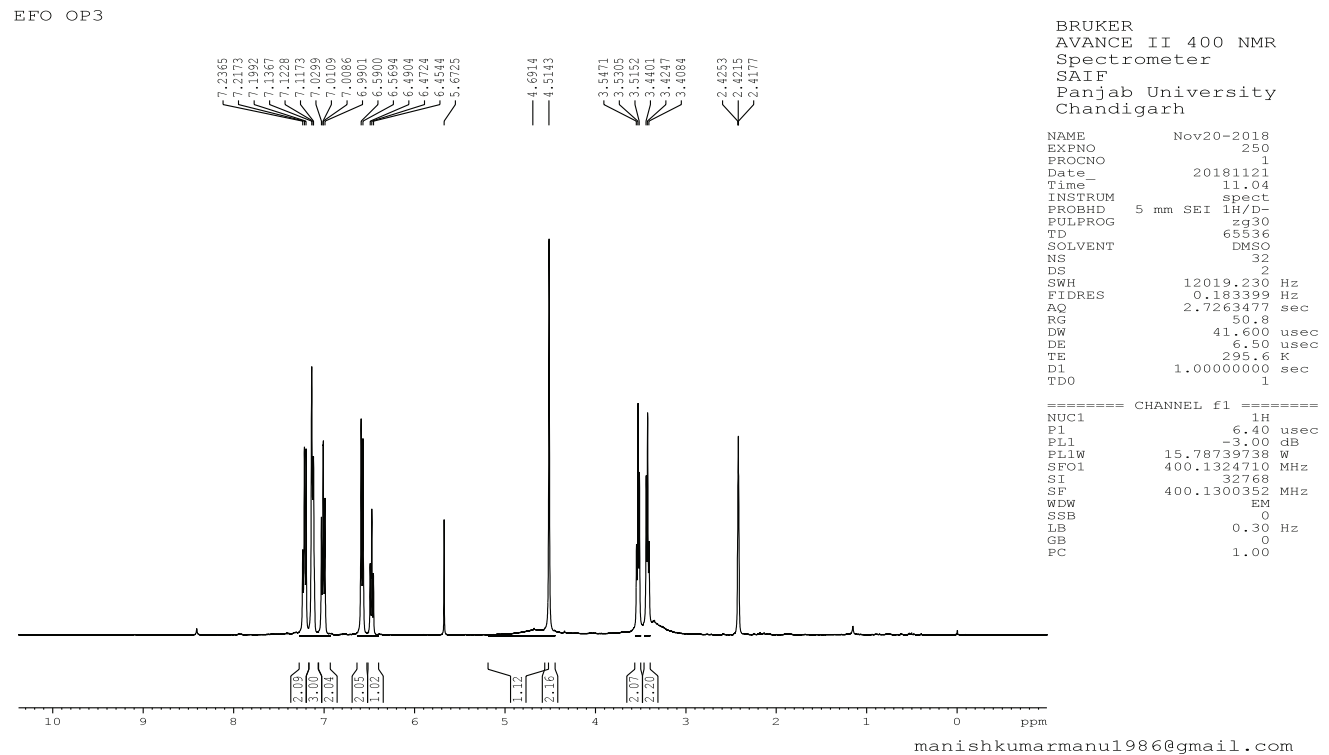


Figure. S13 c . APT spectra of DP1.

Figure. S14 a . ¹H NMR spectra of DP3.

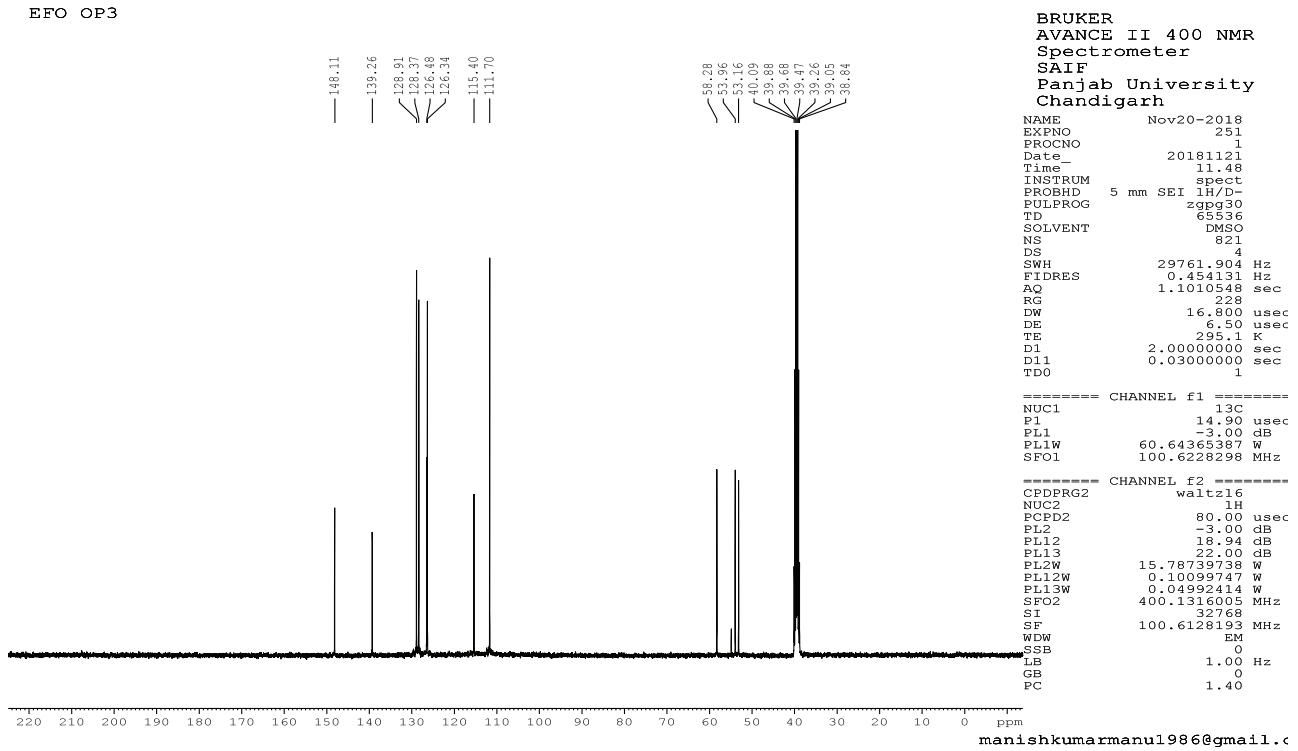


Figure. S14 b. ¹³C NMR spectra of DP3.

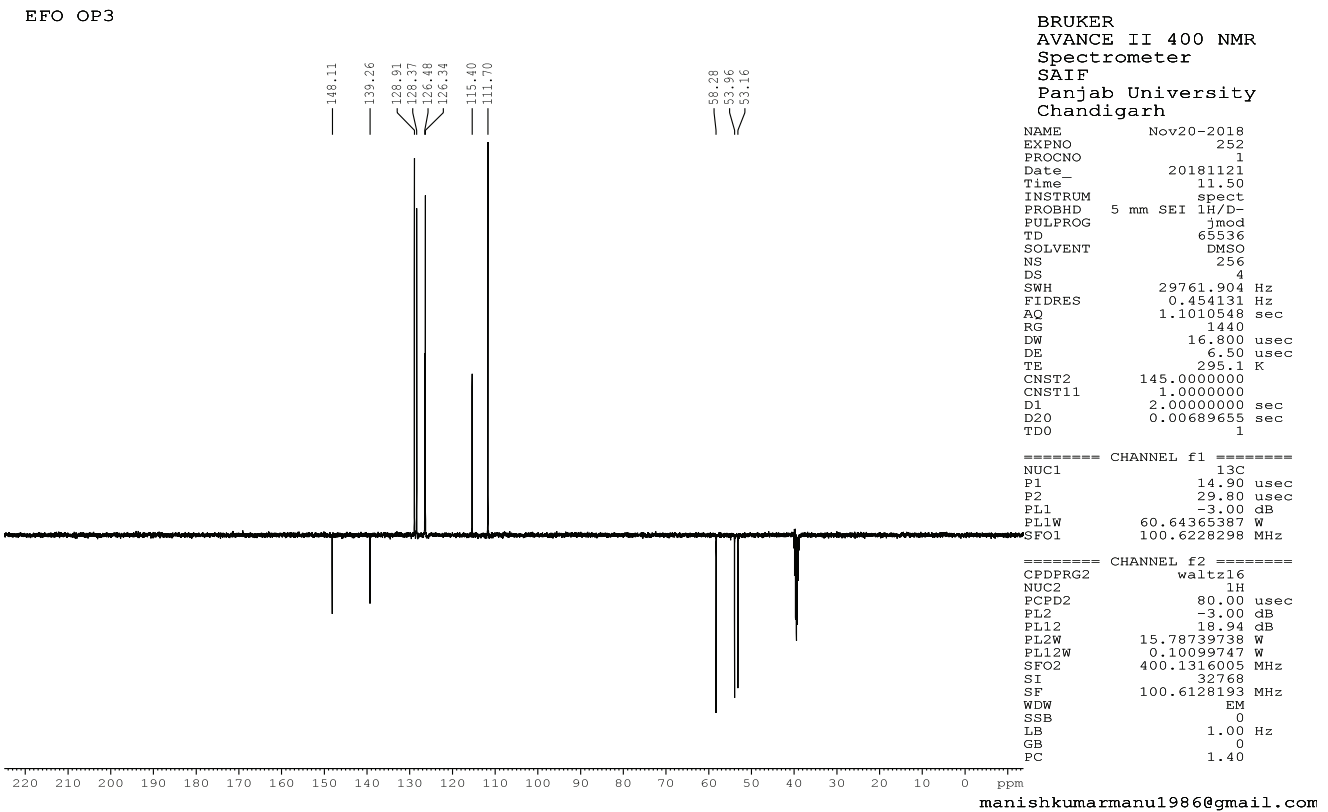
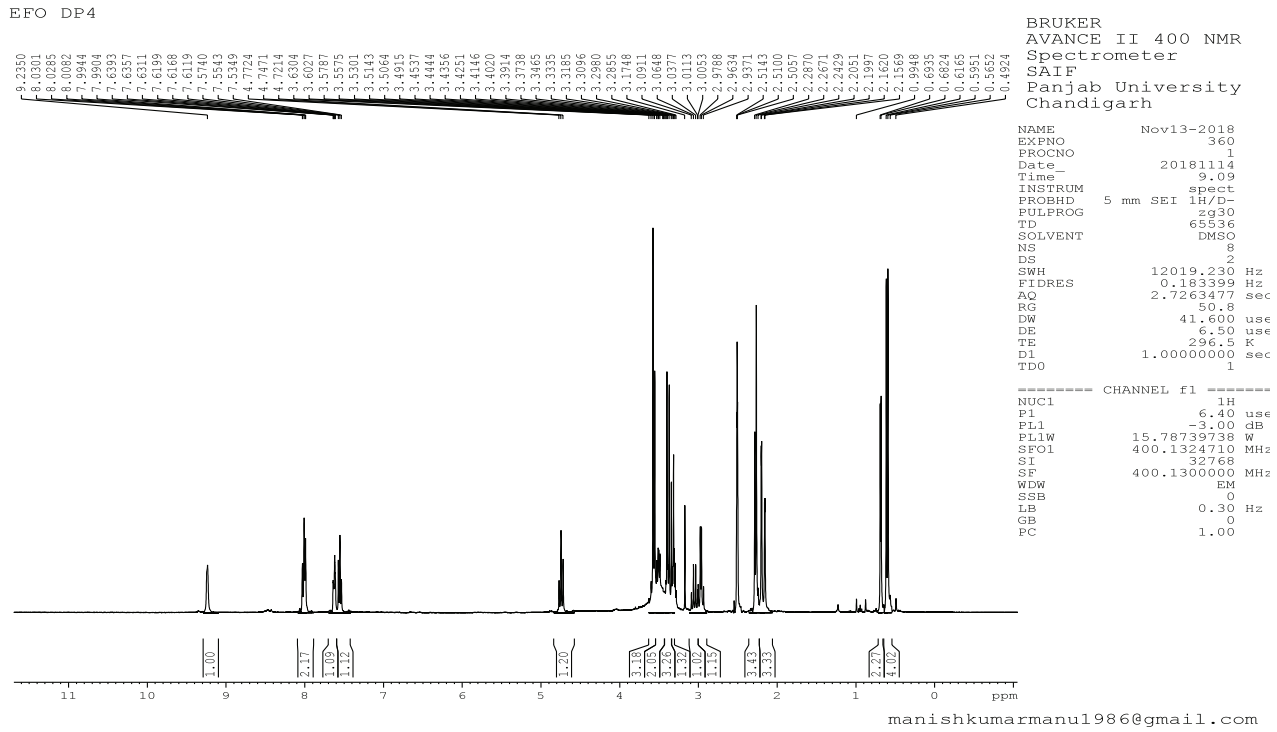
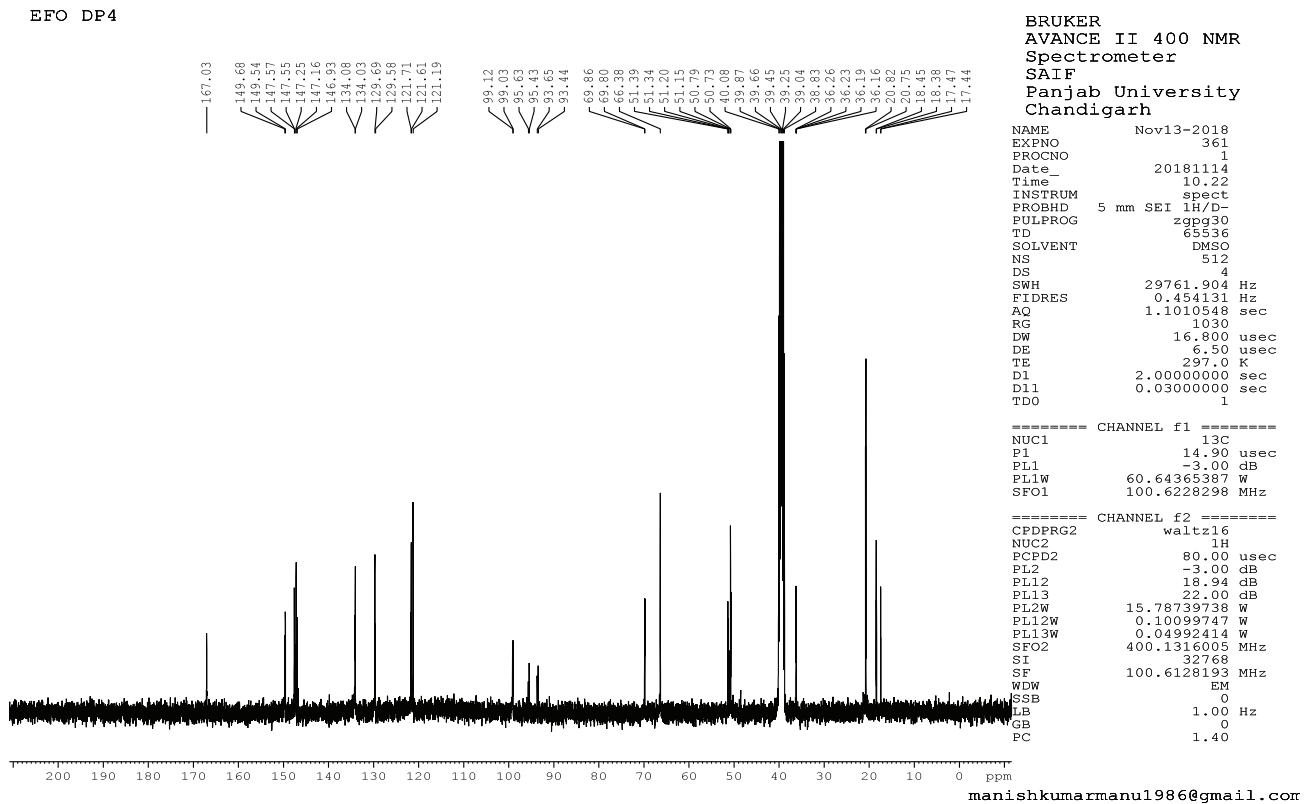


Figure. S14 c. APT spectra of DP3.

Figure. S15 a. ¹H NMR spectra of DP4.Figure. S15 b. ¹³C NMR spectra of DP4.

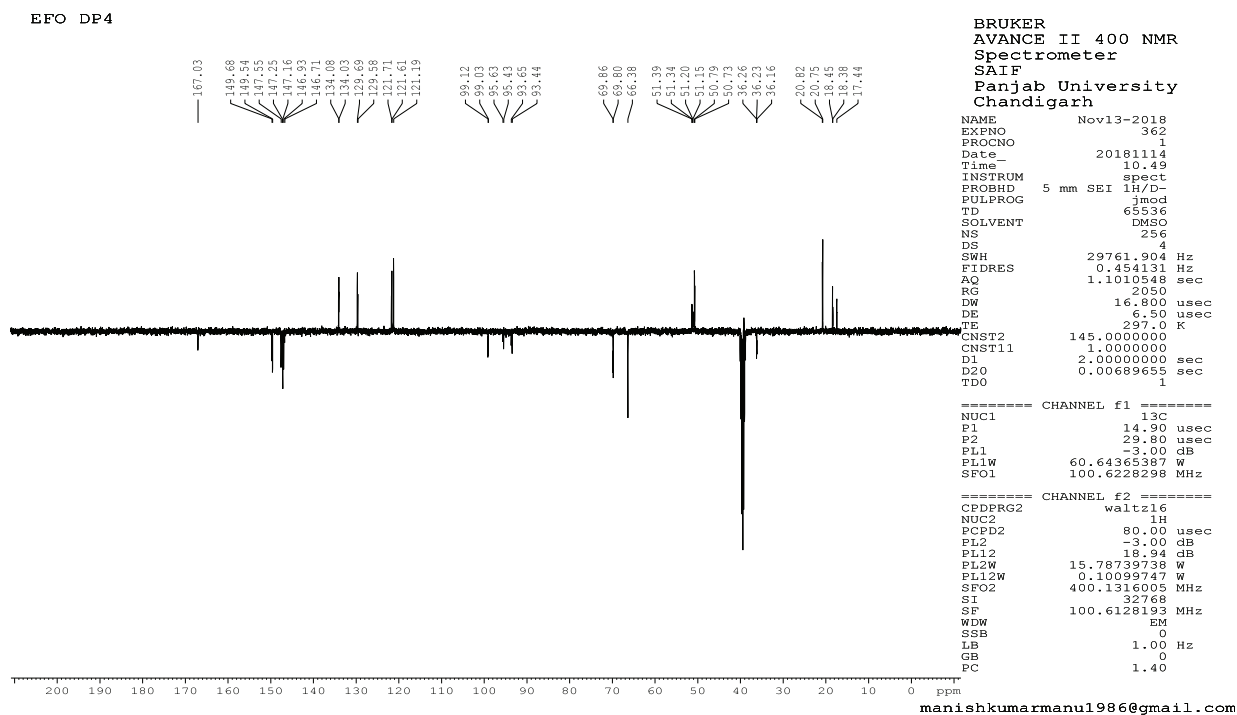
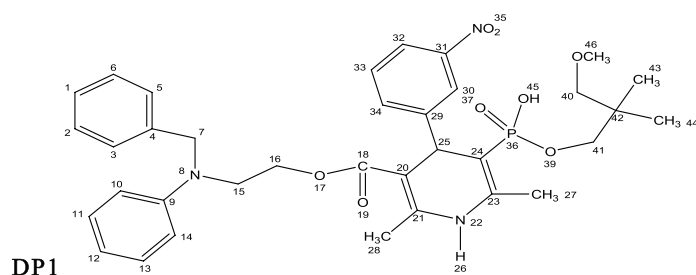


Figure. S15 c. APT spectra of DP4.

Table S1. NMR assignments of EFO.

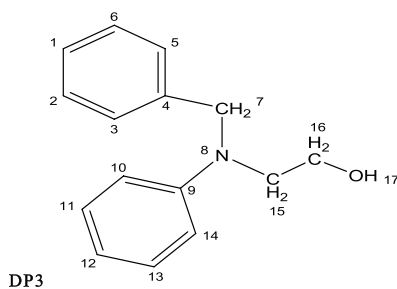
Position	¹ H	Chemical Shift(δ ppm)	Position	¹³ C	APT
22	1H	9.4,s, -NH absent in D2O exchange	18	166.41	Ester
30, 32, 33, 34	4H	8.00-7.98,d, 8.00-7.98,d, 7.52-7.48,t, 7.6-7.58,d, 7.6-7.58,d	1, 2, 3, 5, 6	127.16, 129.09, 129.09, 128.28, 128.28	Aromatic -CH-
1, 2, 3, 5, 6	5H	6.9,m,7.1,m,6.9,m, 6.9,m, 7.1,m	9	148.29	Quaternary carbon
10, 11,12, 13, 14	5H	6.3,s,7.1-6.99,m, 6.2,s,7.1-6.99,m, 6.1, s,	4	147.5	Quaternary carbon
25	1H	4.75-4.78,d	10	98.97	Aromatic -CH-
7	2H	4.58,s	11, 12, 13, 14	129.63, 121.4, 129.63, 98.89	Aromatic -CH-
16	2H	4.30-4.22,m	20, 21, 23, 24	98.97, 148.99, 147.67, 92.47	Quaternary carbon
15	2H	4.05-3.99,m	29, 31,	147.50, 148.06	Quaternary carbon
40	2H	4.0 -3.99,m	30, 32, 33,34	121.46, 121.24, 133.88, 133.86	Aromatic -CH-
41	2H	3.70 -3.59,m	40	74.16	-CH2
27	3H	2.27-2.26,d	41	74.10	-CH2
28	3H	2.20,d	16	74.16	-CH2
43	3H	0.93,d	15	60.12	-CH2
44	3H	0.87-0.86,d	7	56.0	-CH2
1'	3H	1.07-1.05,t	42	38.62	Quaternary carbon
2'	2H	3.47-3.42,m	43	21.02	-CH3
3'	-OH	6.72, broad peak	44	21.02	-CH3
			25	18.53	-CH-
			27, 28	17.48, 17.51	-CH3

Table S2. NMR assignments of DP1.



Position	¹ H	Chemical Shift(δ ppm)	Position	¹³ C	APT
22	1H	9.16,s	18	166.64	Ester group
1, 2, 3, 5, 6	5H	7.16-7.13,t, 7.29-7.25,t, 6.60-6.56,t, 7.16-7.14,t, 7.29-7.25,t	1, 2, 3, 5, 6	129.56, 129.56, 126.59, 126.59, 129.56	Aromatic -CH
10, 11, 12, 13, 14	5H	7.10-7.07,t, 7.22-7.18,t, 6.66-6.63,m, 7.10-7.07, t, 6.66-6.63, m	4	138.86	Quaternary carbon
30, 32, 33, 34	1H	8.04-8.00,t, 8.04- 8.00,t, 7.53-7.49,t, 7.62-7.64,d	9	149.47	Quaternary carbon
25	1H	4.81,t	10, 11, 12, 13, 14	115.99, 129.68, 121.20, 129.68, 115.99	Aromatic -CH
7	2H	4.52-4.49,d	20, 21, 23, 24	98.98, 149.63, 147.59, 93.69	Quaternary carbon
16	2H	4.205-4.17, m	29, 31	146.81, 147.67	Quaternary carbon
15	2H	3.66-3.50,m	30, 32, 33, 34	121.68, 121.68, 129.68,134.15	Aromatic -CH-
40	2H	3.55-3.51,m, 3.34-3.31,m	7	49.40	-CH ₂
41	2H	3.07-2.97,m	40	69.89	-CH ₂
27	3H	2.17,m	41	66.41	-CH ₂
28	3H	2.21,m	16	60.52	-CH ₂
43	3H	0.70,d	15	53.79	-CH ₂
44	3H	0.69,d	46	51.35	-CH ₃
45	1H	3.43-3.42,m	42	36.17	Quaternary carbon
46	3H	3.42-3.35,m	25	18.54	-CH-
			43	17.47	-CH ₃
			44	18.49	-CH ₃

Table S3. NMR assignments of DP3.



Position	¹ H	Chemical Shift(δ ppm)	Position	¹³ C	APT
1, 2, 3, 5, 6	5H	7.13-7.11,d, 7.23-7.19,t, 7.02-6.99,t, 7.02-6.99,t, 7.23-7.19,t	9	149.6	Quaternary carbon
10,11, 12, 13, 14	5H	6.59-6.56,d, 7.13-7.11,t, 6.49-6.45,t, 7.13-7.11,t, 6.59-6.56,d	10, 11, 12, 13, 14	111.70, 128.91,115.40, 128.91, 111.70	Aromatic -CH-
17	---	4.69, broad peak	1, 2, 3, 5,6	126.34,128.37, 126.48,126.48, 128.37	Aromatic -CH-
7	2H	4.51,s	4	139.26	Quaternary carbon
15	2H	3.44-3.40,t	16	58.28	-CH ₂
16	2H	3.54-3.51,t	15	53.96	-CH ₂
			7	53.17	-CH ₂

Table S4. NMR assignments of DP4.

DP4

Position	¹ H	Chemical Shift(δ ppm)	Position	¹³ C	APT
7	1H	9.2	3	167.03	Ester
			5, 6, 8, 9	99.12, 149.58, 147.25, 95.63	Quaternary carbon
15, 17, 18, 19	4H	8.0-7.99,t, 8.0-7.99,t, 7.57-7.53,t, 7.63-7.61,t	14, 16	146.71, 149.54	Quaternary carbon
10	1H	4.77-4.72,t	15, 17, 18, 19	121.71, 121.19, 129.6, 135.08	Aromatic -CH-
1	3H	3.63-3.51,t	24	69.86	-CH ₂
24	2H	3.50-3.44,m	25	66.38	-CH ₂
30	3H	3.45-3.35,m	1	51.15	-CH ₃
29	-OH, absent in D ₂ O exchange	3.33-3.28,m	30	51.39	-CH ₃
25	2H	3.0-2.9,m	26	36.16	Quaternary carbon
12	3H	2.28-2.14,d	27	20.75	-CH ₃
13	3H	2.20-2.15,d	28	20.82	-CH ₃
27	3H	0.69-0.68,d	10	18.45	-CH-
28	3H	0.61-0.56,d	12	18.38	-CH ₃
			13	17.44	-CH ₃

Table S5. IR spectral interpretation of EFO, DP1, DP3 and DP4.

EFO		DP1	
Wave number (cm ⁻¹)	Assignments	Wave number (cm ⁻¹)	Assignments
3435	-NH Stretch	3500	-OH stretch
3185, 3083	Aromatic C-H Stretch	3278	-NH Stretch
2967, 2860	Alkyl C-H stretch	3199, 3088, 3064	Aromatic C-H Stretch
1705	Ester C=O stretch	2872	Alkyl C-H stretch
1526, 1494	Aromatic nitro stretch	2444	Broad peak O=P-OH Stretch
1348, 1248	C-N stretch	1705	Ester
1102	P=O stretch	1598, 1574	O=P-OH Stretch
		1528, 1494	Aromatic nitro stretch
		1348, 1179	C-N stretch
DP4		DP3	
Wave number (cm ⁻¹)	Assignments	Wave number (cm ⁻¹)	Assignments
3500 and 3400	Broad peak covering -OH and -NH group	3304	Broad peak -OH
3192, 3166	Aromatic C-H stretch	3000	Aromatic C-H stretch
2951, 2873, 2848	Alkyl C-H stretch	2970	Alkyl stretch
2444	O=P-OH Stretch	1591, 1432	Aromatic C=C Stretch
1740	Ester C=O stretch		
1644, 1628	O=P-OH Stretch	850	Out of plane bending
1530, 1497	Aromatic nitro stretch	640	Out of plane bending
1348, 1280	C-N Stretch		
1053	P=O stretch		